IEEE Access
Multidisciplinary | Rapid Review | Open Access Journal

Received October 11, 2017, accepted November 20, 2017, date of publication November 23, 2017,
date of current version February 14, 2018.

Digital Object Identifier 10.1109/ACCESS.2017.2777102

Space–Time Line Code for Massive MIMO and Multiuser Systems With Antenna Allocation

JINGON JOUNG, (Senior Member, IEEE)
School of Electrical and Electronics Engineering, Chung-Ang University, Seoul 06974, South Korea

Corresponding author: jgjoung@cau.ac.kr

This work was supported by the Basic Science Research Program through the National Research Foundation funded by the Korean Government under Grant 2016R1D1A1B03930250.

ABSTRACT This paper first investigates an M-by-2 massive multiple-input multiple-output (MIMO) system that transmits a single stream is investigated. For this system, we propose a space–time line code (STLC), which is a transmitting and combining (at a receiver) scheme that achieves full spatial diversity. For the STLC, two consecutive (*time*) information symbols are weighted as per channel gains (*space*), combined at each transmit antenna, and transmitted through the M transmit antennas for two consecutive symbol times. With two receive antennas, the STLC receiver simply combines the signals received in the two symbol times and achieves a diversity order of $2M$ (full diversity). We show that the proposed STLC asymptotically achieves the maximum (optimal) received signal-to-noise ratio as M increases with significantly reduced computational complexity compared with the optimal scheme. Because the proposed STLC receiver requires no or partial channel state information, it avoids the issue of massive MIMO channel estimation. Furthermore, the rigorous performance evaluation under spatially correlated and uncertain channel conditions reveals that the proposed STLC achieves comparable or better performance than the existing schemes, and the results verify that the proposed STLC scheme is a potential candidate for M-by-2 massive MIMO systems. Next, the transmit antenna allocation algorithms are devised for a multiuser STLC system. Each user achieves full diversity order from the corresponding MIMO channels after the antenna allocation. The signal-to-interference-plus-noise ratio (SINR) of each user is analyzed considering the multiuser interference and channel uncertainty, and its lower bound is derived. Using the SINR lower bound, greedy algorithms that allocate the transmit antennas are devised. Rigorous simulation demonstrates that multiuser STLC with the proposed antenna allocation is robust against channel uncertainty and can improve the average SINR, improving the quality of experience. Furthermore, it is observed that the proposed STLC with antenna allocation method achieves the best performance if M is sufficiently large. The results in this paper show that the STLC can be a potential candidate for an M-by-2 (multiuser) massive MIMO systems.

INDEX TERMS Space–time line code, spatial-diversity gain, multiuser, massive MIMO.

I. INTRODUCTION

Recently, a new scheme to achieve full spatial diversity, called the space–time line code (STLC), was proposed for a multiple-input multiple-output (MIMO) system with M transmit and two/three/four receive antennas [1]. In an STLC transmitter, two consecutive (*time*) information symbols are weighted by channel gains (*space*) and combined before transmission. The two STLC symbols are then transmitted through M transmit antennas and simply combined at the receiver, thus achieving full spatial diversity. The interest in STLC stems primarily from the fact that it allows for simple combining without the knowledge of channel state information (CSI) at the receiver; thus, it relieves the receiver from the complexity burden required for estimating the CSI and decoding the STLC transmissions that achieve full diversity. Particularly, in time-division duplex (TDD) systems, a low-complexity system design is possible when the STLC scheme is operated with a space–time block code (STBC) scheme in transmitter [2]–[5] and receiver pair, by reducing the frequency of channel estimations and allowing the easier channel estimation to be used at the receiver [1]. Also, the STLC can be used for improving secrecy capacity as shown in [6].

From the study on full-spatial-diversity schemes including maximum ratio combining (MRC) [7]–[11], maximum ratio transmission (MRT), STBC [2]–[5], and STLC [1], the

full-spatial-diversity systems that achieve a diversity order of $2M$ using $2M$-spatial channels are characterized according to their system configurations (i.e., the number of antennas and CSI availability) as follows:

- MRC: $1 \times 2M$ CSI is available at the receiver (Rx) only.
- MRT: $2M \times 1$ CSI is available at the transmitter (Tx) only.
- STBC: $2 \times M$ CSI is available at the Rx only.
- STLC: $M \times 2$ CSI is available at the Tx only.

In this paper, we consider an M-by-2 massive MIMO system with STLC, which achieves the full diversity order of $2M$, and compare it with an M-by-2 system employing MRT and MRC (MRTC) at the transmitter and receiver, respectively. Because the MRTC system needs to estimate the channels at the receiver with two antennas and this requires at least M orthogonal pilot symbols or training sequences, which may be intractable if M is exceedingly large, i.e., the case of massive MIMO systems [12]–[14]. In particular, the estimation of the large-dimensional channels is a one of challenging issues on massive MIMO systems [14], [15].

We first provide a formal expression for M-by-2 STLC and derive the analytical signal-to-noise ratio (SNR) of the STLC systems. The STLC receiver, without knowing the CSI, provides a significant advantage over an MRTC system. With the relaxed CSI requirement and less computational complexity at the receiver, the STLC system achieves a bit-error-rate (BER) performance comparable to that of the MRTC system. For further rigorous comparison, we consider maximum eigen beamforming (MEB) for an M-by-2 system with CSI at both Tx and Rx, which is the optimal scheme in terms of the received SNR [16]. We analytically show that the M-by-2 STLC system asymptotically achieves an identical SNR to that of MEB as M increases, which is also numerically verified by comparing the received SNRs and BERs. Furthermore, we analytically and numerically investigate the spatial correlation effect on the received SNR. One important observation from the results is that the transmit antenna correlation, which is typically high in a massive antenna transmitter, does not considerably affect system performance. On the other hand, we analytically show that the received SNR of the STLC marginally increases as the receive antenna correlation increases, and we also numerically verify this analysis. From the numerical simulation, we observe that the STLC performance is as robust against channel uncertainty as MRTC, while MEB is relatively very sensitive.

Next, the massive MIMO STLC is applied to a system that supports multiple users (i.e., receivers). A method for the allocation of the transmit antennas to users is proposed for a multiuser STLC in order to improve the average signal-to-interference-plus-noise ratio (SINR) and quality-of-experience (QoE). Antenna allocation, in which all transmit antennas are activated, is different from antenna selection [17]–[19], which uses a partial set of antennas. Each user achieves full-spatial-diversity order from the allocated transmit antennas. The SINR of each user is analyzed considering the multiuser interference and channel uncertainty, and its lower bound is derived. Using the SINR lower bound, two greedy-based *antenna allocation* algorithms are devised. Rigorous simulation validates that the multiuser STLC with the proposed antenna allocation is robust against channel uncertainty and can improve the average SINR and QoE. Moreover, it is observed that the STLC with antenna allocation achieves the best performance if the number of transmit antenna is sufficiently large. In conclusion, the STLC scheme is attractive for a practical massive MIMO system.

The rest of the paper is organized as follows. In Section II, an STLC scheme for an M-by-2 massive MIMO system is formally expressed and its received SNR is derived. Section III describes MRTC and MEB and compares their received SNR to that of STLC. In Section IV, spatial correlation is considered. Section V provides analytical and numerical results under channel uncertainty. In Section VI, a multiuser STLC system is proposed with greedy-based antenna allocation algorithms. Section VII concludes this paper.

Notation: The superscripts T, H, and $*$ denote transposition, Hermitian transposition, and complex conjugate, respectively, for any scalar, vector or matrix; E stands for expectation of a random variable x; for any scalar x, vector $\boldsymbol{x}$, and matrix $\boldsymbol{X}$, the notations $|x|$, $\|\boldsymbol{x}\|$, and $\|\boldsymbol{X}\|_F$ denote the absolute value of x, the two norm of $\boldsymbol{x}$, and the Frobenius-norm of $\boldsymbol{X}$, respectively; $\boldsymbol{X}^{1/2}$ is the principal square root of the square matrix $\boldsymbol{X}$, i.e., $\boldsymbol{X}^{1/2}\boldsymbol{X}^{1/2} = \boldsymbol{X}$; $|\mathcal{X}|$ represents the cardinality of set $\mathcal{X}$; $\mathcal{X} \setminus \mathcal{Y}$ is the set of elements in set $\mathcal{X}$ but not in set $\mathcal{Y}$; $\mathcal{X} \cup \mathcal{Y}$ is the set of elements in set $\mathcal{X}$ or set $\mathcal{Y}$; $\emptyset$ denotes an empty set; and $x \sim \mathcal{CN}(0, \sigma^2)$ means that a complex random variable x conforms to a normal distribution with a zero mean and variance σ^2.

II. STLC FOR M-BY-2 MASSIVE MIMO SYSTEMS

The STLC scheme in [1] is precisely generalized to a system with M transmit and two receive antennas, as depicted in Fig. 1. The notations of channel gains for $M \times 2$ STLC are listed in Table 1. Channel $h_{n,m}$ represents independent channel gain from transmit antenna m to receive antenna n, where $m \in \mathcal{M} = \{1, \ldots, M\}$ and $n \in \{1, 2\}$. The sum of all channel gains is denoted by γ_M and is expressed as

$$\gamma_M = \sum_{m=1}^{M} |h_{1,m}|^2 + |h_{2,m}|^2. \tag{1}$$

The M-by-2 STLC encoding and transmission methods at the Tx and a received STLC signal combining method at the Rx are first introduced. The received SNR analysis is then provided.

A. ENCODING AND TRANSMISSION SEQUENCE

Let x be an information symbol that conforms to the complex normal distribution with $\mathrm{E}[|x|^2] = \sigma_x^2$, i.e., $\mathcal{CN}(0, \sigma_x^2)$. Two STLC symbols denoted by $s_{m,1}$ and $s_{m,2}$ are transmitted via transmit antenna m during the first and second symbol periods, respectively. Using the CSI at the transmitter (refer to [1, Sec. V] for the scenario how to get the CSI at the

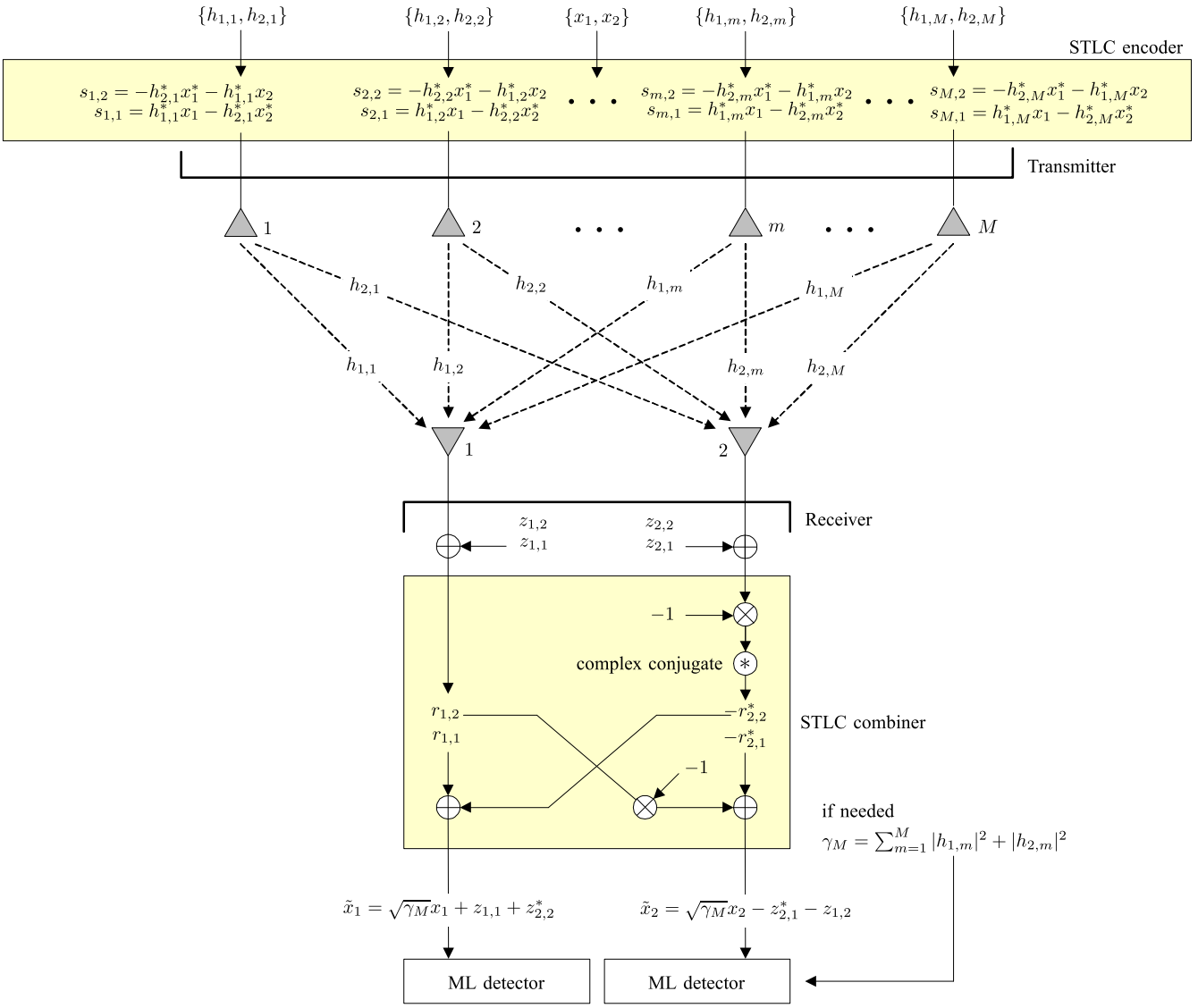

FIGURE 1. Example of a new full-diversity achieving $M \times 2$ STLC system that achieves full diversity, where a Type-15 structure with an STLC encoding matrix $C_{(1,2)}^{d}$ in [1, Table IV] is used for the encoding and combining at the transmitter and receiver, respectively.

TABLE 1. Definition of channels, $h_{n,m}$, between transmit antenna m and receive antenna n.

	Tx antenna m
Rx antenna $n = 1$	$h_{1,m}$
Rx antenna $n = 2$	$h_{2,m}$

TABLE 2. Encoding and transmit sequence for the STLC Scheme with M-transmit antennas.

	Tx antenna m
Tx time $t = 1$	$s_{m,1} = h_{1,m}^* x_1 - h_{2,m}^* x_2^*$
Tx time $t = 2$	$s_{m,2} = -h_{2,m}^* x_1^* - h_{1,m}^* x_2$

transmitter), the STLC symbols $s_{m,1}$ and $s_{m,2}$ are encoded by combining two information symbols x_1 and x_2, which are weighted by channel gains, for example, as follows:

$$s_{m,1} = h_{1,m}^* x_1 - h_{2,m}^* x_2^*, \quad \forall m \in \mathcal{M} \tag{2a}$$
$$s_{m,2} = -h_{2,m}^* x_1^* - h_{1,m}^* x_2, \quad \forall m \in \mathcal{M}. \tag{2b}$$

The encoding in (2a) is represented by a vector-and-matrix form as

$$\begin{bmatrix} s_{m,1} \\ s_{m,2}^* \end{bmatrix} = \begin{bmatrix} h_{1,m}^* & -h_{2,m}^* \\ -h_{2,m} & -h_{1,m} \end{bmatrix} \begin{bmatrix} x_1 \\ x_2^* \end{bmatrix}. \tag{3}$$

Here, for simplicity and tractable analysis later, we assume that all users use a Type-**15** structure with an STLC encoding matrix $\boldsymbol{C}_{(1,2)}^{d}$ in [1, Table IV]. Note that any type of STLC matrix and structure in [1, Table IV] can be applied to (2a). The STLC symbols in (2a) are listed in Table 2.

At transmission time 1, an STLC symbol $s_{m,1}$ is transmitted through the mth transmit antenna for all $m \in \mathcal{M}$, simultaneously. In the subsequent transmission time 2, an STLC symbol $s_{m,2}$ is transmitted through the mth transmit antenna

TABLE 3. Notation for STLC received signal $r_{n,t}$.

	Rx time $t=1$	Rx time $t=2$
Rx antenna $n=1$	$r_{1,1}$	$r_{1,2}$
Rx antenna $n=2$	$r_{2,1}$	$r_{2,2}$

for all $m \in \mathcal{M}$, simultaneously. To satisfy, without loss of generality (w.l.o.g), the transmit power constraint by σ_x^2, the transmitter weights (normalizes) $s_{m,t}$ with η. The normalization factor η can be readily derived as $\eta = 1/\sqrt{\gamma_M}$, such that $\sum_{m=1}^{M} \mathrm{E}\,|\eta s_{m,t}|^2 = \sigma_x^2$ for all t.

Denote the received signal at receive antenna n at time t by $r_{n,t}$ as shown in Table 3. The receive symbols with two receive antennas can then be expressed as follows:

$$r_{1,1} = \frac{1}{\sqrt{\gamma_M}}\left(\sum_{m=1}^{M} h_{1,m}s_{m,1}\right) + z_{1,1} \tag{4a}$$

$$r_{1,2} = \frac{1}{\sqrt{\gamma_M}}\left(\sum_{m=1}^{M} h_{1,m}s_{m,2}\right) + z_{1,2} \tag{4b}$$

$$r_{2,1} = \frac{1}{\sqrt{\gamma_M}}\left(\sum_{m=1}^{M} h_{2,m}s_{m,1}\right) + z_{2,1} \tag{4c}$$

$$r_{2,2} = \frac{1}{\sqrt{\gamma_M}}\left(\sum_{m=1}^{M} h_{2,m}s_{m,2}\right) + z_{2,2} \tag{4d}$$

where $z_{n,t}$ is an additive white Gaussian noise (AWGN) with zero mean and σ_z^2 variance in the received signal $r_{n,t}$.

As depicted in Fig. 1 and defined in (2a), the STLC encoding is performed separately on each transmit antenna. This parallel encoding enables high-speed processing at the Tx with massive antennas.

B. COMBINING SCHEME

The STLC combiner is shown in Fig. 1. Directly combining $\{r_{1,1}, r_{1,2}, r_{2,1}, r_{2,2}\}$ in (4a) as $(r_{1,1} - r_{2,2}^*)$ and $(-r_{2,1}^* - r_{1,2})$, the STLC receiver obtains the weighted estimates of symbols as follows:

$$\begin{aligned} r_{1,1} - r_{2,2}^* &= \frac{1}{\sqrt{\gamma_M}}\left(\sum_{m=1}^{M} h_{1,m}\left(h_{1,m}^* x_1 - h_{2,m}^* x_2^*\right)\right) \\ &\quad - \frac{1}{\sqrt{\gamma_M}}\left(\sum_{m=1}^{M} h_{2,m}^*\left(-h_{2,m}^* x_1^* - h_{1,m}^* x_2\right)^*\right) \\ &\quad + z_{1,1} - z_{2,2}^* \\ &= \frac{1}{\sqrt{\gamma_M}}\sum_{m=1}^{M}\left(|h_{1,m}|^2 + |h_{2,m}|^2\right)x_1 + z_{1,1} - z_{2,2}^* \\ &= \sqrt{\gamma_M}x_1 + z_{1,1} - z_{2,2}^* \end{aligned} \tag{5a}$$

$$\begin{aligned} -r_{2,1}^* - r_{1,2} &= -\frac{1}{\sqrt{\gamma_M}}\left(\sum_{m=1}^{M} h_{2,m}^*\left(h_{1,m}^* x_1 - h_{2,m}^* x_2^*\right)^*\right) \\ &\quad - \frac{1}{\sqrt{\gamma_M}}\left(\sum_{m=1}^{M} h_{1,m}\left(-h_{2,m}^* x_1^* - h_{1,m}^* x_2\right)\right) \\ &\quad - z_{2,1}^* - z_{1,2} \\ &= \frac{1}{\sqrt{\gamma_M}}\sum_{m=1}^{M}\left(|h_{1,m}|^2 + |h_{2,m}|^2\right)x_2 - z_{2,1}^* - z_{1,2} \\ &= \sqrt{\gamma_M}x_2 - z_{2,1}^* - z_{1,2}. \end{aligned} \tag{5b}$$

As seen in (5a), the STLC receiver does not need full CSI to combine the received signals, which we call *blind combining* [1]; however, it needs an effective channel gain $\sqrt{\gamma_M}$ for maximum likelihood (ML) detection in subsequent processing. The effective channel gain can be estimated by using the blind SNR estimation techniques (see [20] and references therein). Note that, for phase-shift-keying (PSK) symbol detection, even $\sqrt{\gamma_M}$ is not required.

C. RECEIVED SNR OF STLC

Note that $(z_{1,1} - z_{2,2}^*) \sim \mathcal{CN}(0, 2\sigma_z^2)$ and $(-z_{2,1}^* - z_{1,2}) \sim \mathcal{CN}(0, 2\sigma_z^2)$ in (5a) because the sum of the two independent AWGNs is also AWGN. Thus, the resulting SNR after the blind combining in (5a) is readily derived as follows:

$$\mathrm{SNR}_{STLC} = \frac{\gamma_M \sigma_x^2}{2\sigma_z^2}. \tag{6}$$

From (6), we verify that the $M \times 2$ STLC system achieves the diversity order of $2M$ (refer to [1]), i.e., full diversity gain, and half the full array processing gain, i.e., $2M/2 = M$. The factor of two in the denominator in (6) comes from the fact that the two AWGNs are directly combined at the receiver, as shown in (5a).

III. COMPARISON OF STLC WITH MRTC AND MEB

In order to introduce models of benchmakring systems, i.e., MRTC and MEB, the spatial channels defined in Table 1 are represented in the matrix form as follows:

$$\boldsymbol{H} = \begin{bmatrix} \boldsymbol{h}_1 \\ \boldsymbol{h}_2 \end{bmatrix} = \begin{bmatrix} h_{1,1} & h_{1,2} & \cdots, & h_{1,M} \\ h_{2,1} & h_{2,2} & \cdots, & h_{2,M} \end{bmatrix} \in \mathbb{C}^{2\times M} \tag{7}$$

where $\boldsymbol{h}_1 \in \mathbb{C}^{1\times M}$ and $\boldsymbol{h}_2 \in \mathbb{C}^{1\times M}$ represent the first and second row vectors of $\boldsymbol{H}$.

A. RECEIVED SNR OF MRTC

Suppose, w.l.o.g., that $\|\boldsymbol{h}_1\| \geq \|\boldsymbol{h}_2\|$. Then, the transmitter generates the weight vector of the larger-norm channel vector for MRT [21], [22] as follows:

$$\boldsymbol{w} = \frac{\boldsymbol{h}_1^H}{\|\boldsymbol{h}_1\|}. \tag{8}$$

After the MRT, the received signal at the receiver becomes

$$\boldsymbol{r} = \begin{bmatrix} \|\boldsymbol{h}_1\| \\ \boldsymbol{h}_2\boldsymbol{h}_1^H/\|\boldsymbol{h}_1\| \end{bmatrix} x + \boldsymbol{z} \tag{9}$$

where $\boldsymbol{z} = [z_{1,1}\ z_{2,1}]^T$ is an AWGN vector. Now, the receiver applies MRC with two received signals to achieve the maximum SNR as follows [7]:

$$\frac{1}{\sigma_z}\begin{bmatrix}\|\boldsymbol{h}_1\| \\ \boldsymbol{h}_2\boldsymbol{h}_1^H/\|\boldsymbol{h}_1\|\end{bmatrix}^H \boldsymbol{r} = \frac{\|\boldsymbol{h}_1\|^2 + \boldsymbol{h}_1\boldsymbol{h}_2^H\boldsymbol{h}_2\boldsymbol{h}_1^H/\|\boldsymbol{h}_1\|^2}{\sigma_z}x + \frac{1}{\sigma_z}\begin{bmatrix}\|\boldsymbol{h}_1\| \\ \boldsymbol{h}_2\boldsymbol{h}_1^H/\|\boldsymbol{h}_1\|\end{bmatrix}^H \boldsymbol{z}. \quad (10)$$

From (10), the SNR of MRTC is generally derived as follows (the proof is tedious and omitted in this paper):

$$\mathrm{SNR}_{MRTC} = \left(\|\boldsymbol{h}_{max}\|^2 + \frac{|\boldsymbol{h}_2\boldsymbol{h}_1^H\boldsymbol{h}_1\boldsymbol{h}_2^H|}{\|\boldsymbol{h}_{max}\|^2}\right)\frac{\sigma_x^2}{\sigma_z^2} \quad (11)$$

where $\|\boldsymbol{h}_{max}\| = \max_{n\in\{1,2\}}\|\boldsymbol{h}_n\|$.

B. RECEIVED SNR OF MEB

For comparison of single data stream transmitting systems, an MEB method is considered. For single date stream transmission, the MEB performs beamforming through one channel vector that corresponds to the maximum singular value of a channel matrix; thus, it is optimal in terms of the received SNR [16].

The MIMO channel in (7) is decomposed by singular value decomposition (SVD) as follows:

$$\boldsymbol{H} = \begin{bmatrix}\boldsymbol{u}_1 & \boldsymbol{u}_2\end{bmatrix}\begin{bmatrix}d_1 & 0 & \boldsymbol{0}_{1,M-2} \\ 0 & d_2 & \boldsymbol{0}_{1,M-2}\end{bmatrix}\begin{bmatrix}\boldsymbol{v}_1 & \cdots & \boldsymbol{v}_M\end{bmatrix}^H \quad (12)$$

where d_k is the kth largest singular value of $\boldsymbol{H}$; $\boldsymbol{u}_k$ and $\boldsymbol{v}_k$ are the left and right singular vectors, respectively, which correspond to d_k ($k \in \{1, 2\}$); and $\boldsymbol{0}_{1,M-2}$ is a 1-by-$(M-2)$ zero vector. The optimal eigen beamforming vector is then $\boldsymbol{v}_1$ and the corresponding receive combining vector is $\boldsymbol{u}_1^H$, such that the effective channel gain is maximized by d_1 as follows:

$$\boldsymbol{u}_1^H\boldsymbol{r} = \boldsymbol{u}_1^H(\boldsymbol{H}\boldsymbol{v}_1x + \boldsymbol{z}) = d_1x + \boldsymbol{u}_1^H\boldsymbol{z} = d_1x + z' \quad (13)$$

where $\boldsymbol{r} = [r_{1,1}\ r_{2,1}]^T$ is the received signal vector at antennas 1 and 2 (see Table 3). Here, note that there is no transmit power normalization factor because $\boldsymbol{v}_1$ is a unit-norm vector, i.e., $\mathrm{E}(\|\boldsymbol{v}_1x\|^2) = \mathrm{E}(x^*\boldsymbol{v}_1^H\boldsymbol{v}_1x) = \sigma_x^2$. Further, because $\mathrm{E}[z'(z')^*] = \mathrm{E}[\boldsymbol{u}_1^H\boldsymbol{z}\boldsymbol{z}^H\boldsymbol{u}_1] = \boldsymbol{u}_1^H\,\mathrm{E}[\boldsymbol{z}\boldsymbol{z}^H]\boldsymbol{u}_1 = \boldsymbol{u}_1^H\begin{bmatrix}\sigma_z^2 & 0 \\ 0 & \sigma_z^2\end{bmatrix}\boldsymbol{u}_1 = \sigma_z^2$, z' conforms to the same distribution as z, i.e., $z' \sim \mathcal{CN}(0, \sigma_z^2)$. Therefore, from (13), the received SNR of MEB is derived as

$$\mathrm{SNR}_{MEB} = \frac{d_1^2\sigma_x^2}{\sigma_z^2}. \quad (14)$$

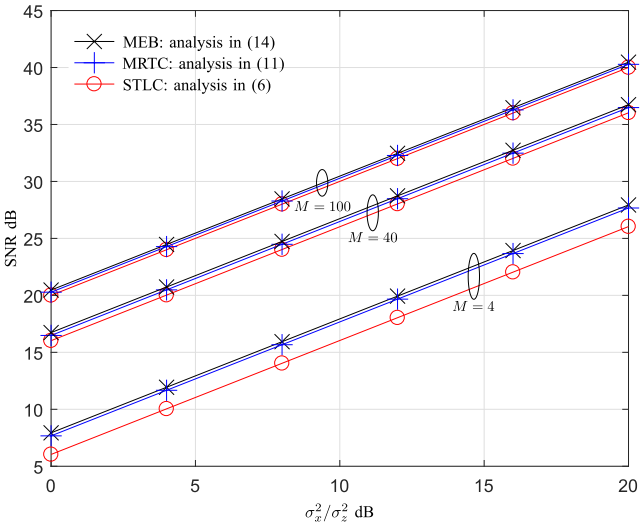

FIGURE 2. Analytic SNR comparison over σ_x^2/σ_z^2 for $M = \{4, 40, 100\}$.

C. SNR GAP ANALYSIS BETWEEN AN STLC SCHEME AND AN OPTIMUM SCHEME MEB

From (6) and (14), the gap between STLC's SNR and optimal scheme MEB's SNR, denoted by Δ, is derived as

$$\Delta \triangleq \mathrm{SNR}_{MEB} - \mathrm{SNR}_{STLC} = \frac{d_1^2\sigma_x^2}{\sigma_z^2} - \frac{\gamma_M\sigma_x^2}{2\sigma_z^2} \overset{(a)}{=} \frac{(d_1^2 - d_2^2)\sigma_x^2}{2\sigma_z^2} \geq 0 \quad (15)$$

where (a) follows that $\gamma_M = \|\boldsymbol{H}\|_F^2 = d_1^2 + d_2^2$.

For asymptotic intuition, the following theorem on extreme singular values is applied to (15).

Theorem 1: Condition number of complex Gaussian matrices [23]: For an $n \times m$ ($n \leq m$) complex Gaussian random matrix $\boldsymbol{A}$ with independent and identically distributed (i.i.d.) elements that are $\mathcal{CN}(0, 1)$, its condition number κ converges almost surely to $\frac{1+\sqrt{y}}{1-\sqrt{y}}$ as $m \to \infty$, where n depends on m in such a way that $\lim_{m\to\infty} n/m = y \in [0, 1]$. Moreover,

$$\mathrm{E}\log\kappa = \log\frac{1+\sqrt{y}}{1-\sqrt{y}} + \mathcal{O}(1), \text{ as } m \to \infty. \quad (16)$$

From Theorem 1, we can readily get the following corollary:

Corollary 1: The gap between STLC's SNR and MEB's SNR vanishes as the number of transmit antennas M increases.

Proof: Applying Theorem 1 to our system configuration, we can easily show that the condition number of $\boldsymbol{H}$ goes to one as M goes to infinity, because $\lim_{M\to\infty} 2/M = 0$. This implies that $d_2 \to d_1$ and $y = 0$ in (16). As a consequence, Δ in (15) approaches zero. ■

D. RECEIVED SNR AND BER EVALUATION

The received SNRs of STLC, MRTC, and MEB derived in (6), (11), and (14), respectively, are numerically compared in Fig. 2. The analytical SNRs are compared

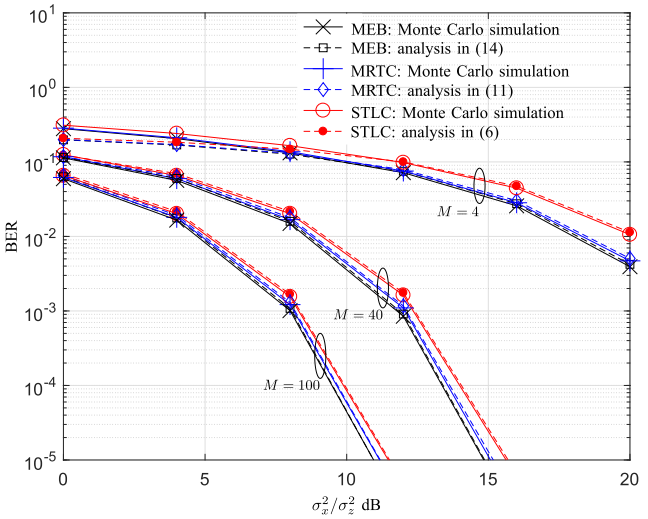

FIGURE 3. BER performance comparison over σ_x^2/σ_z^2 when $M = \{4, 40, 100\}$ and 256-QAM is used.

over σ_x^2/σ_z^2. As expected, all SNRs increase as σ_x^2/σ_z^2 increases. By varying the number of transmit antennas M from 4 to 100, we observe that the SNR gap between STLC and MEB also decreases and the SNR of STLC approaches that of MEB as stated in Corollary 1.

For further verification of our analyses, in Fig. 3, analytical BERs are compared with BERs obtained from Monte Carlo simulation. The analytical BER performance is obtained using $BER \approx 0.5Q(\sqrt{3\mathrm{SNR}/255})$ for 256-quadratic amplitude modulation (QAM) [24] with analytic SNRs in (6), (11), and (14), where $Q(\cdot)$ is a Q-function defined as $Q(x) = \frac{1}{\sqrt{2\pi}}\int_x^\infty exp\left(\frac{-u^2}{2}\right)du$. When $M = 4$ and σ_x^2/σ_z^2 is low, there is a non-negligible discrepancy between the analytical and Monte Carlo simulation results due to BER approximation. In general, the analytically derived BER matches well with the BER obtained from Monte Carlo simulation regardless of M and σ_x^2/σ_z^2. Further, we can observe that the BER gap between STLC and MEB decreases as M increases. From the results, SNR analyses are verified and Corollary 1 is further validated.

E. COMPUTATIONAL COMPLEXITY AND REQUIRED INFORMATION

The required computational complexity for the STLC, MRTC, and MEB schemes and the required CSI at the Tx and Rx are compared.

1) STLC

For STLC encoding, $4M$ multiplications and $2M$ additions of complex values are required. For STLC decoding, two additions of complex values are required. Thus, the total complexity order is $\mathcal{O}(M)$, which is the first order of polynomial complexity. While full CSI is required at an STLC Tx, only the effective channel gain γ_M, which can be readily measured from the received signal strength, is required at an STLC Rx unless PSK modulation is used.

2) MRTC

From (8) and (10), it is obvious that the complexity order of MRTC is $\mathcal{O}(M)$, which is the same as the STLC. For the MRT in (8), full CSI is required at an MRTC Tx. For the MRC in (10), the full CSI is also required at the MRCT Rx.

3) MEB

Either MEB Tx or Rx needs to perform SVD of an M-by-2 complex matrix for pre- or post-processing (beamforming). The SVD complexity is a bottleneck of the computational complexity in the MEB system and its order is $\mathcal{O}(M^3)$ [25]. Indeed full CSI is required at both MEB Tx and Rx.

IV. SPATIALLY CORRELATED CHANNELS

In this section, we consider the effect of the spatial correlation of channels. The massive MIMO channels could be highly spatially correlated, especially at the transmitter owing to the large number of antennas within the limited space [26]–[28].

An M-by-2 spatially correlated MIMO channel matrix is modeled as

$$\boldsymbol{H}_c = \left[\boldsymbol{h}_{c,1}^T\ \boldsymbol{h}_{c,2}^T\right]^T = \boldsymbol{R}_{rx}^{1/2}\boldsymbol{H}\boldsymbol{R}_{tx}^{1/2} \tag{17}$$

where $\boldsymbol{H} \in \mathbb{C}^{M\times 2}$ consists of i.i.d complex Gaussian random variables with a mean of zero and a variance of one; the Rx and Tx correlation matrices are modeled as $\boldsymbol{R}_{rx} = \mathrm{toeplitz}([\rho_{rx}^0\ \rho_{rx}^1])$ and $\boldsymbol{R}_{tx} = \mathrm{toeplitz}([\rho_{tx}^0\ \rho_{tx}^1 \cdots \rho_{tx}^{M-1}])$ [29]; and ρ_{rx} and ρ_{tx} are the correlation factors at Rx and Tx, respectively, which are between zero (uncorrelated) and one (perfectly correlated). Using this correlated channel model, we investigated the received SNRs of STLC, MRTC, and MEB.

A. RECEIVED SNR OF STLC

Applying the spatial correlation model to (2a)–(4a), the diversity gain factor in the received SNR in (6) is modified as follows:

$$\begin{aligned}\gamma_M' &= \|\boldsymbol{H}_c\|_F^2 = \|\boldsymbol{R}_{rx}^{1/2}\boldsymbol{H}\boldsymbol{R}_{tx}^{1/2}\|_F^2 \\ &= \mathrm{tr}\left(\boldsymbol{R}_{rx}^{1/2}\boldsymbol{H}\boldsymbol{R}_{tx}^{1/2}(\boldsymbol{R}_{tx}^{1/2})^H\boldsymbol{H}^H(\boldsymbol{R}_{rx}^{1/2})^H\right) \\ &= \mathrm{tr}\left(\boldsymbol{H}\boldsymbol{R}_{tx}\boldsymbol{H}^H\boldsymbol{R}_{rx}\right) \\ &= \mathrm{tr}\left(\begin{bmatrix}\boldsymbol{h}_1\\ \boldsymbol{h}_2\end{bmatrix}\boldsymbol{R}_{tx}\begin{bmatrix}\boldsymbol{h}_1^H & \boldsymbol{h}_2^H\end{bmatrix}\begin{bmatrix}\boldsymbol{r}_{rx,1}\\ \boldsymbol{r}_{rx,2}\end{bmatrix}\right) \\ &= \mathrm{tr}\left(\begin{bmatrix}\boldsymbol{h}_1\boldsymbol{R}_{tx}(\boldsymbol{h}_1^H\boldsymbol{r}_{rx,1}+\boldsymbol{h}_2^H\boldsymbol{r}_{rx,2}) \\ \boldsymbol{h}_2\boldsymbol{R}_{tx}(\boldsymbol{h}_1^H\boldsymbol{r}_{rx,1}+\boldsymbol{h}_2^H\boldsymbol{r}_{rx,2})\end{bmatrix}\right)\end{aligned} \tag{18}$$

where $\boldsymbol{r}_{rx,1}$ and $\boldsymbol{r}_{rx,2}$ are the first and second row vectors of $\boldsymbol{R}_{rx}$, respectively. From the definitions that $\boldsymbol{r}_{rx,1} = [1\ \rho_{rx}]$ and $\boldsymbol{r}_{rx,2} = [\rho_{rx}\ 1]$, γ_M' in (18) can be further derived as follows:

$$\begin{aligned}\gamma_M' &= \boldsymbol{h}_1\boldsymbol{R}_{tx}\boldsymbol{h}_1^H + \boldsymbol{h}_2\boldsymbol{R}_{tx}\boldsymbol{h}_2^H + \rho_{rx}(\boldsymbol{h}_1\boldsymbol{R}_{tx}\boldsymbol{h}_2^H + \boldsymbol{h}_2\boldsymbol{R}_{tx}\boldsymbol{h}_1^H) \\ &= \boldsymbol{h}_1\boldsymbol{R}_{tx}\boldsymbol{h}_1^H + \boldsymbol{h}_2\boldsymbol{R}_{tx}\boldsymbol{h}_2^H + 2\rho_{rx}\,\mathrm{Re}(\boldsymbol{h}_1\boldsymbol{R}_{tx}\boldsymbol{h}_2^H) \\ &= \mathrm{tr}\left(\boldsymbol{R}_{tx}(\boldsymbol{h}_1^H\boldsymbol{h}_1 + \boldsymbol{h}_2^H\boldsymbol{h}_2)\right) + 2\rho_{rx}\,\mathrm{Re}(\boldsymbol{h}_1\boldsymbol{R}_{tx}\boldsymbol{h}_2^H) \\ &= \mathrm{tr}(\boldsymbol{R}_{tx}\boldsymbol{H}^H\boldsymbol{H}) + 2\rho_{rx}\,\mathrm{Re}(\boldsymbol{h}_1\boldsymbol{R}_{tx}\boldsymbol{h}_2^H).\end{aligned} \tag{19}$$

Substituting γ_M in (6) with γ'_M in (19), the SNR of STLC under spatially correlated channel conditions is expressed as a function of ρ_{tx} and ρ_{rx} as follows:

$$\mathsf{SNR}_{STLC}(\rho_{tx}, \rho_{rx}) = \frac{\left(\mathrm{tr}(\boldsymbol{R}_{tx}\boldsymbol{H}^H\boldsymbol{H}) + 2\rho_{rx}\,\mathrm{Re}(\boldsymbol{h}_1\boldsymbol{R}_{tx}\boldsymbol{h}_2^H)\right)\sigma_x^2}{2\sigma_z^2}. \quad (20)$$

From (20), we see that the SNR of STLC is a decreasing function of ρ_{tx} because as ρ_{tx} increases, the Toeplitz matrix $\boldsymbol{R}_{tx}$ becomes more dispersive (i.e., the magnitude of off-diagonal terms increases) and does not capture the strong channel gains located on the diagonal of a diagonal dominant matrix $\boldsymbol{H}^H\boldsymbol{H}$. On the other hand, because $\mathrm{tr}(\boldsymbol{R}_{tx}\boldsymbol{H}^H\boldsymbol{H}) \gg 2\rho_{rx}\,\mathrm{Re}(\boldsymbol{h}_1\boldsymbol{R}_{tx}\boldsymbol{h}_2^H)$, ρ_{rx} does not considerably affect the SNR of STLC.

B. RECEIVED SNR OF MRTC

Applying the spatial correlation model to (11), the effective SNR of MRTC is derived as

$$\mathsf{SNR}_{MRTC} = \left(\|\boldsymbol{h}_{c,max}\|^2 + \frac{\left|\boldsymbol{h}_{c,2}\boldsymbol{h}_{c,1}^H\boldsymbol{h}_{c,1}\boldsymbol{h}_{c,2}^H\right|}{\|\boldsymbol{h}_{c,max}\|^2}\right)\frac{\sigma_x^2}{\sigma_z^2} \quad (21)$$

where $\|\boldsymbol{h}_{c,max}\| = \max_{n\in\{1,2\}}\|\boldsymbol{h}_{c,n}\|$; the correlated channel vectors are written as

$$\boldsymbol{h}_{c,1} = \rho_1\boldsymbol{h}'_1 + \rho_2\boldsymbol{h}'_2 \quad (22a)$$
$$\boldsymbol{h}_{c,2} = \rho_2\boldsymbol{h}'_1 + \rho_1\boldsymbol{h}'_2 \quad (22b)$$
$$\boldsymbol{h}'_1 \triangleq \boldsymbol{h}_1\boldsymbol{R}_{tx}^{1/2} \quad (22c)$$
$$\boldsymbol{h}'_2 \triangleq \boldsymbol{h}_2\boldsymbol{R}_{tx}^{1/2} \quad (22d)$$

and the correlation factors ρ_1 and ρ_2 are obtained from the receive antenna correlation factor ρ_{rx}, such that $\rho_1^2 + \rho_2^2 = 1$ and $2\rho_1\rho_2 = \rho_{rx}$. Substituting (22a) in (21), we can express (21) as a function of ρ_{tx} and ρ_{rx} as follows (the proof is tedious and omitted):

$$\mathsf{SNR}_{MRTC}(\rho_{tx}, \rho_{rx}) = \left(\alpha + \frac{\beta}{\alpha}\right)\frac{\sigma_x^2}{\sigma_z^2} \quad (23)$$

where

$$\alpha = \left(\frac{1+\sqrt{1-\rho_{rx}^2}}{2}\right)\|\boldsymbol{h}'_{max}\|^2 + \left(\frac{1-\sqrt{1-\rho_{rx}^2}}{2}\right)\|\boldsymbol{h}'_{\overline{max}}\|^2 + \rho_{rx}\,\mathrm{Re}\left(\boldsymbol{h}'_1(\boldsymbol{h}'_2)^H\right) \quad (24a)$$

$$\beta = \frac{\rho_{rx}^2}{4}\|\boldsymbol{H}'\|_F^4 + \rho_{rx}\|\boldsymbol{H}'\|_F^2\,\mathrm{Re}\left(\boldsymbol{h}'_1\boldsymbol{h}'_2\right) + \frac{\rho_{rx}^2}{2}\,\mathrm{Re}\left(\boldsymbol{h}'_1(\boldsymbol{h}'_2)^H\boldsymbol{h}'_1(\boldsymbol{h}'_2)^H\right) + \left(1-\frac{\rho_{rx}^2}{2}\right)\left|\boldsymbol{h}'_1(\boldsymbol{h}'_2)^H\right|^2 \quad (24b)$$

and $\boldsymbol{H}' = \boldsymbol{H}\boldsymbol{R}_{tx}^{1/2}$.

If we scrutinize (23), interestingly, the SNR of MRTC is proportional to ρ_{rx}. This is because α decreases with the dominant order $o(\rho_{rx})$, while β increases with the dominant order $o(\rho_{rx}^2)$, which increases faster than the decreasing speed of α; therefore, $\mathsf{SNR}_{MRTC}(\rho_{tx}, \rho_{rx}) = o(\rho_{rx})^{-1} + o(\rho_{rx})o(\rho_{rx}^2)$, where $o(\rho)$ is an increasing function over ρ.

On the other hand, the SNR of MRTC is inversely proportional to ρ_{tx} because both $\|\boldsymbol{h}'\|$ and $\|\boldsymbol{H}\|_F$ decrease as ρ_{tx} increases, and as a consequence, both α and β decrease. Here, it is apparent that β decreases much faster than α.

C. RECEIVED SNR OF MEB

As spatial correlation factors ρ_{tx} and ρ_{rx} increase, the condition number of the correlated channel matrix $\boldsymbol{H}_c$ in (17) increases [30] and enhances the principal eigenmode of the channel at the cost of the remaining eigenmodes, i.e., d_1 increases, while d_2 decreases [31]. Therefore, the SNR of MEB in (14) increases as ρ_{tx} and/or ρ_{rx} increase.

D. ANALYSES VERIFICATION AND DISCUSSION

In Fig. 4(a), SNRs are evaluated over the transmit antenna correlation, i.e., ρ_{tx}, when $M = 100$, $\sigma_x^2/\sigma_z^2 = 8$ dB, and the receive antenna correlation factor ρ_{rx} is fixed by 0.1. The SNRs of STLC and MRTC obtained from analyses in (20) and (23) are compared with those obtained from the Monte Carlo simulation. From the results, the SNR analyses under spatially correlated channel conditions are verified. The SNRs of MEB and MRTC increase as ρ_{tx} increases. On the other hand, as analyzed in (20), the SNR of STLC decreases as ρ_{tx}; however, the variation is very subtle. In Fig. 4(b), for further verification, the BERs are evaluated. Obviously, the inversely proportional relationship between the SNR and the BER is observed. The numerical results reveal that M-by-2 massive MIMO systems using MEB, MRTC, or the proposed STLC are insensitive to the spatial correlation between transmit antennas.

Similarly, the receive antenna correlation effect is investigated by evaluating SNRs and BERs in Fig. 5. In Fig. 5(a), SNRs are evaluated over the receive antenna correlation, i.e., ρ_{rx}, when $M = 100$, $\sigma_x^2/\sigma_z^2 = 8$ dB, and the transmit antenna correlation factor ρ_{tx} is fixed by 0.4. Comparing the SNRs of STLC and MRTC obtained from analyses in (20) and (23) with those obtained from the Monte Carlo simulation, we verify the SNR analyses. The SNRs of MEB and MRTC significantly increase as ρ_{rx} increases, while the SNR of STLC is again almost stable regardless of ρ_{rx}, as stated in Section IV.B. In Fig. 5(b), an inversely proportional relationship between the SNR and BER is clearly observed. The numerical results reveal that the M-by-2 massive MIMO systems using MEB and MRTC are sensitive to receive antenna correlation; however, those using the proposed STLC are insensitive. Because the spatial correlation between two receive antennas is insignificant, focusing on the low ρ_{rx} regime, the performance of the proposed STLC is comparable to those of MEB and MRTC.

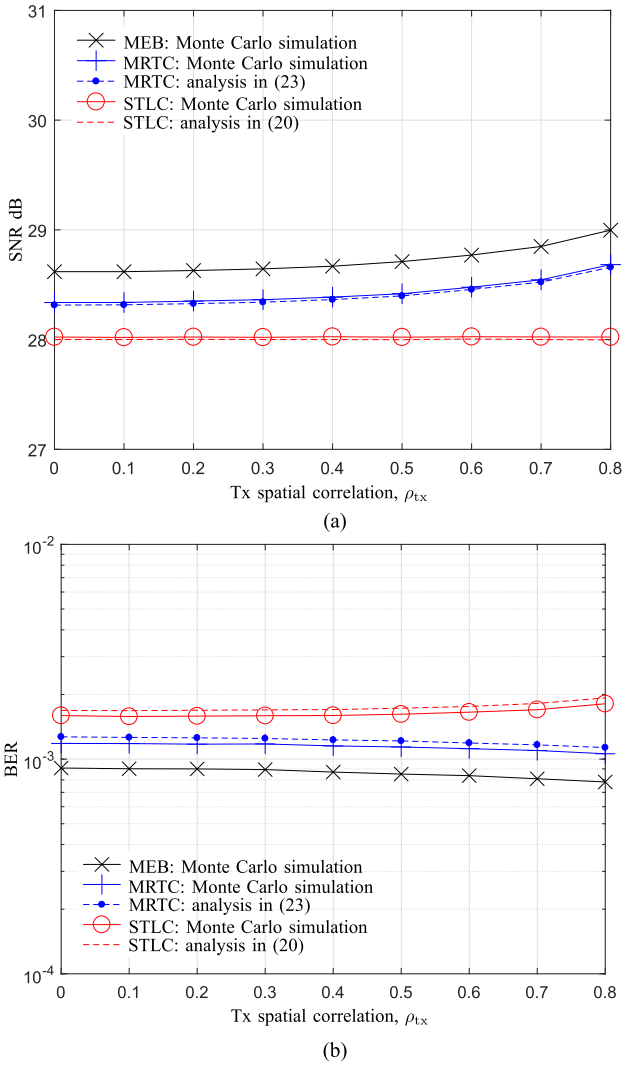

FIGURE 4. Performance comparison over ρ_{tx} when $M = 100$, $\sigma_x^2/\sigma_z^2 = 8$ *dB*, $\rho_{rx} = 0.1$, and 256-QAM is used. (a) SNR. (b) BER.

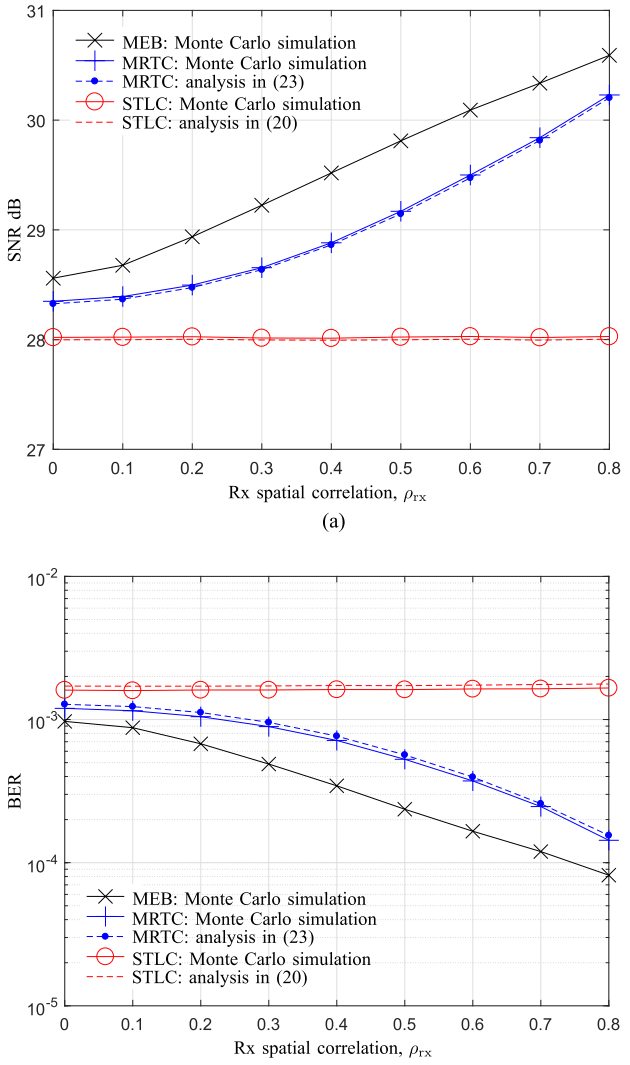

FIGURE 5. Performance comparison over ρ_{rx} when $M = 100$, $\sigma_x^2/\sigma_z^2 = 8$ *dB*, $\rho_{tx} = 0.4$, and 256-QAM is used. (a) SNR. (b) BER.

V. CHANNEL UNCERTAINTY

The CSI at a transmitter could be outdated because, in practice, the CSI is obtained from channel estimation in the previous receiving mode, i.e., the time varying channel in TDD system. Further, considering the estimation error, the mismatch of channel calibration in the TDD systems, and a feedback error in frequency-division duplex systems, the CSI uncertainty is inevitable.

We denote an estimated (outdated) CSI at the transmitter by $\tilde{h} \triangleq h + \epsilon$, where h is the actual (current) channel element and ϵ is the estimation error. Assuming that the estimation errors of all channel elements are independent of one another and they conform to normal distribution with mean zero and variance σ_ϵ^2, we represent a mean-squared error (MSE) of the estimation by σ_ϵ^2, i.e., $\mathrm{E}\,|h - \tilde{h}|^2 = \sigma_\epsilon^2$ [1]. We derive, w.l.o.g., the SNR of STLC under channel uncertainty from the estimate of x_1 (a similar procedure can be applied x_2 to obtain the same result.).

Applying the channel uncertainty to (2a) and (4a), the estimate (5a) is rewritten as follows:

$$\begin{aligned} & r_{1,1} - r_{2,2}^* \\ &= \widetilde{\gamma}_M^{-1/2} \sum_{m=1}^{M} h_{1,m} s_{m,1} - \widetilde{\gamma}_M^{-1/2} \sum_{m=1}^{M} h_{2,m}^* s_{m,2}^* \\ &\quad + z_{1,1} - z_{2,2}^* \\ &= \widetilde{\gamma}_M^{-1/2} \sum_{m=1}^{M} h_{1,m} \left(\tilde{h}_{1,m}^* x_1 - \tilde{h}_{2,m}^* x_2^* \right) + \widetilde{\gamma}_M^{-1/2} \\ &\quad \times \sum_{m=1}^{M} h_{2,m}^* \left(\tilde{h}_{2,m} x_1 + \tilde{h}_{1,m} x_2^* \right) + z_{1,1} - z_{2,2}^* \\ &= \widetilde{\gamma}_M^{-1/2} \Bigg(\gamma_M x_1 + \sum_{m=1}^{M} \left(h_{1,m} \epsilon_{1,m}^* + h_{2,m}^* \epsilon_{2,m} \right) x_1 \\ &\quad + \sum_{m=1}^{M} \left(h_{2,m}^* \epsilon_{1,m} - h_{1,m} \epsilon_{2,m}^* \right) x_2^* \Bigg) + z_{1,1} - z_{2,2}^* \end{aligned} \tag{25}$$

where $\tilde{\gamma}_M = \sum_{m=1}^{M} |\tilde{h}_{1,m}|^2 + |\tilde{h}_{2,m}|^2$ is the sum of all channel gains, which is estimated at Tx and Rx.

Then, from (25), we obtain the estimate of x_1 as follows:

$$\begin{aligned}\tilde{x}_1 &= \tilde{\gamma}_M^{-1/2}(r_{1,1} - r_{2,2}^*) \\ &= \gamma_M \tilde{\gamma}_M^{-1} x_1 + \tilde{\gamma}_M^{-1} \sum_{m=1}^{M} \left(h_{1,m}\epsilon_{1,m}^* + h_{2,m}^* \epsilon_{2,m}\right) x_1 \\ &\quad + \tilde{\gamma}_M^{-1} \sum_{m=1}^{M} \left(h_{2,m}^* \epsilon_{1,m} - h_{1,m}\epsilon_{2,m}^*\right) x_2^* \\ &\quad + \tilde{\gamma}_M^{-1/2}(z_{1,1} - z_{2,2}^*). \end{aligned} \tag{26}$$

Again, note that instead of full CSI, only $\tilde{\gamma}_M$ is required at the STLC receiver (denoted by Scenario 1), and even it is not required if PSK constellation is used.

From (26), the SNR of STLC under uncertain channel presence is then derived as a function of channel uncertainty σ_ϵ^2 as

$$\mathrm{SNR}_{STLC}(\sigma_\epsilon^2) = \mathrm{E}\left(\frac{|x_1|^2}{|\tilde{x}_1 - x_1|^2}\right) \tag{27}$$

and its lower bound is derived using Jensen's inequality as follows (the detailed derivation is omitted here):

$$\begin{aligned}&\mathrm{SNR}_{STLC}(\sigma_\epsilon^2) \\ &\geq \frac{(\gamma_M + 2M\sigma_\epsilon^2)^2 \sigma_x^2}{2(2M^2\sigma_\epsilon^4\sigma_x^2 + \sigma_\epsilon^2\gamma_M\sigma_x^2 + (\gamma_M + 2M\sigma_\epsilon^2)\sigma_z^2)}. \end{aligned} \tag{28}$$

Note that, for $\sigma_\epsilon^2 = 0$, the SNR bound in (28) is identical to (6).

If the effective channel gain $\gamma_M/\sqrt{\tilde{\gamma}_M}$ in (25) is perfectly estimated at the receiver by using additional pilot symbols (denoted by Scenario 2), the estimate (26) is given by

$$\begin{aligned}\tilde{x}_1 &= \sqrt{\tilde{\gamma}_M}/\gamma_M (r_{1,1} - r_{2,2}^*) \\ &= x_1 + \gamma_M^{-1} x_1 \sum_{m=1}^{M} \left(h_{1,m}\epsilon_{1,m}^* + h_{2,m}^* \epsilon_{2,m}\right) x_1 \\ &\quad + \gamma_M^{-1} \sum_{m=1}^{M} \left(h_{2,m}^* \epsilon_{1,m} - h_{1,m}\epsilon_{2,m}^*\right) x_2^* \\ &\quad + \sqrt{\tilde{\gamma}_M}/\gamma_M (z_{1,1} - z_{2,2}^*) \end{aligned} \tag{29}$$

and from it the received SNR is derived as follows:

$$\mathrm{SNR}_{STLC}(\sigma_\epsilon^2) = \frac{\gamma_M^2 \sigma_x^2}{2(\gamma_M\sigma_x^2\sigma_\epsilon^2 + (\gamma_M + 2M\sigma_\epsilon^2)\sigma_z^2)} \tag{30}$$

which is a general expression of the received SNRs in [1], where the SNRs are shown for $M = 1$ and $M = 2$.

In Figs. 6 and 7, the BER performance for a 256-QAM transmission is evaluated in Scenarios 1 and 2, respectively, over the channel uncertainty σ_ϵ^2 when $\sigma_x^2/\sigma_z^2 = 8$ *dB*. From the simulation results, the received SNR lower bounds of STLC in (28) and (30), i.e., the upper bound of BER, are verified. As observed, the bound becomes tight as M increases. Moreover, we also observe that the proposed STLC is more robust against CSI uncertainty than MEB and MRTC,

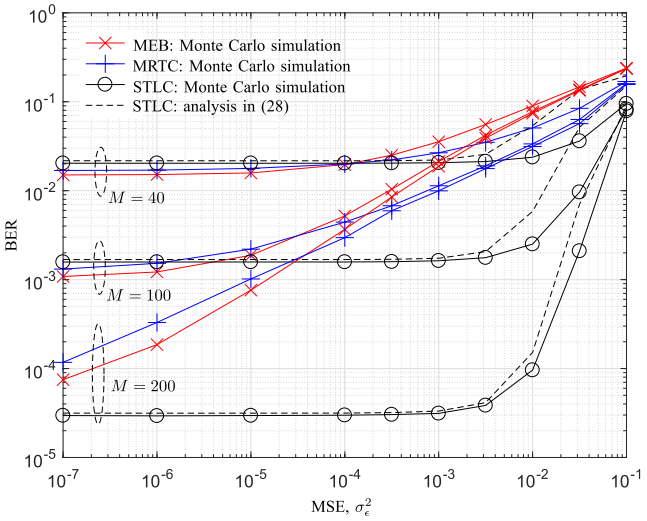

FIGURE 6. BER performance comparison in scenario 1 over MSE of channel estimation, i.e., σ_ϵ^2 when 256-QAM is used and $\sigma_x^2/\sigma_z^2 = 8$ *dB*.

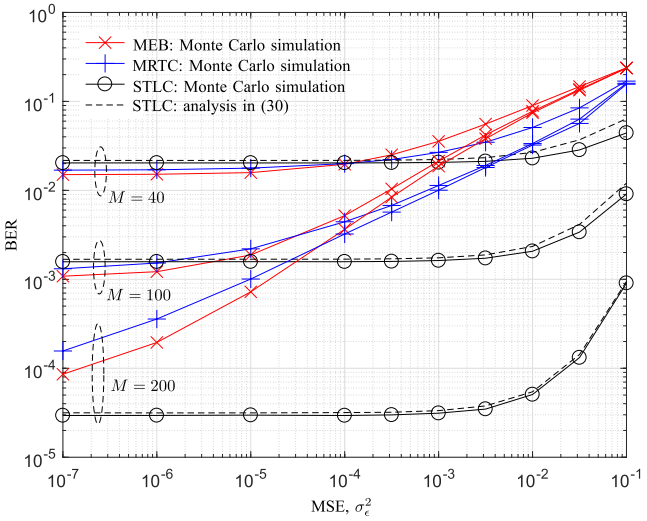

FIGURE 7. BER performance comparison in scenario 2 over MSE of channel estimation, i.e., σ_ϵ^2 when 256-QAM is used and $\sigma_x^2/\sigma_z^2 = 8$ *dB*.

especially when M is large. Though the MEB achieves optimal performance when CSI is perfect, it is very vulnerable for CSI uncertainty and provides a severely poor performance with the uncertain CSI.

As the first part of this study, we investigated M-by-2 massive MIMO systems that transmit a single stream, as summarized in Table 4.

VI. MULTIUSER APPLICATION

The STLC scheme is applied to support U multiple users (receivers), as depicted in Fig. 8, where one STLC transmitter with M transmit antennas supports U users, each of which has two receive antennas. We denote the user index by u and its set by $\mathcal{U}$, i.e., $u \in \mathcal{U} = \{1, \ldots, U\}$. The notations used for the channel gains are shown in Table 5. Channel $h_{n,u,m}$ represents independent channel gain from

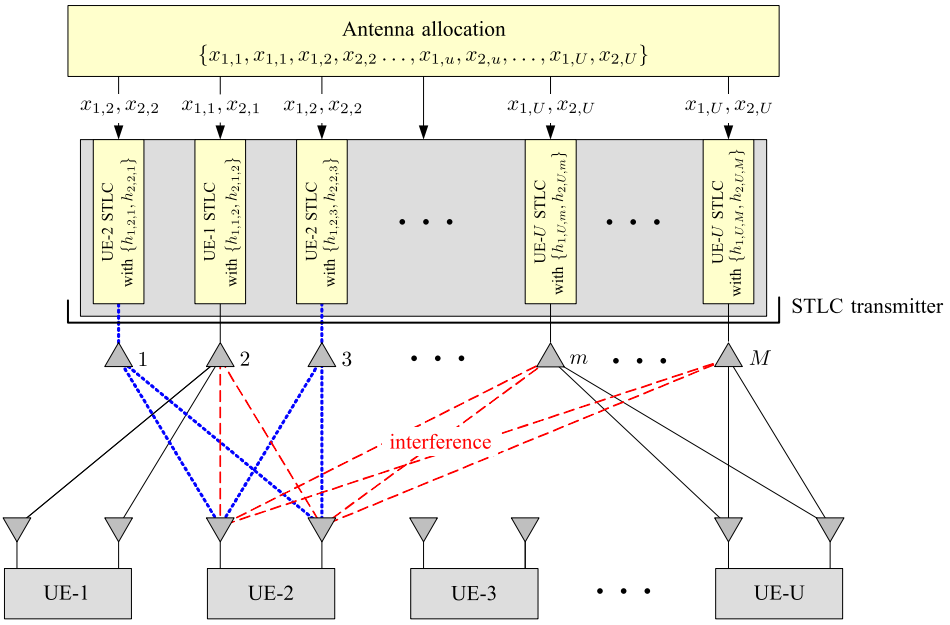

FIGURE 8. Antenna allocation example of the proposed $M \times 2$ STLC system achieving full diversity with U users.

TABLE 4. Summary of the comparison of M-by-2 MRTC, MEB, and STLC schemes, with respect to computational complexity, required information, spatial correlation effect (ρ: ρ_{tx} and ρ_{rx}), and CSI Uncertainty (MSE of CSI, σ_ϵ^2).

	MRTC	MEB	STLC
Complexity order	$\mathcal{O}(M)$	$\mathcal{O}(M^3)$	$\mathcal{O}(M)$
Required info. at Tx	$\boldsymbol{H}$	$\boldsymbol{H}$	$\boldsymbol{H}$
Required info. at Rx	$\boldsymbol{H}$	$\boldsymbol{H}$	none or γ_M
BER when $\rho = \sigma_\epsilon^2 = 0$	comparable	best	comparable $\xrightarrow{M\to\infty}$ best
BER as ρ_{tx} increases	stable	stable	stable
BER as ρ_{rx} increases	decreases	decreases	stable
CSI uncertainty	vulnerable	vulnerable	robust

TABLE 5. Definition of channel $h_{n,u,m}$ between receive antenna n of user u and allocated transmit antenna m.

	Tx antenna m
Rx antenna $n = 1$ at user u	$h_{1,u,m}$
Rx antenna $n = 2$ at user u	$h_{2,u,m}$

TABLE 6. Encoding and Transmit Sequence for STLC Scheme at Transmit Antenna m for User u.

	Tx antenna m
Tx time $t = 1$	$s_{m,1} = h_{1,u,m}^* x_{1,u} - h_{2,u,m}^* x_{2,u}^*$
Tx time $t = 2$	$s_{m,2} = -h_{2,u,m}^* x_{1,u}^* - h_{1,u,m}^* x_{2,u}$

transmit antenna m to receive antenna n of user u. To support multiple STLC users, a transmit antenna set is allocated to each user, which is possible because the STLC encoding is performed individually across transmit antennas, as shown in Section II. Here, the antenna set allocated to user u is denoted by $\mathcal{M}_u$. Then, the maximum diversity gain that can be achieved by user u is denoted by γ_u and written as follows:

$$\gamma_u = \sum_{m\in\mathcal{M}_u} |h_{1,u,m}|^2 + |h_{2,u,m}|^2 = \sum_{m\in\mathcal{M}_u} \|\boldsymbol{h}_{u,m}\|^2 \quad (31)$$

where $\boldsymbol{h}_{u,m}$ is the 2-by-1 channel vector between transmit antenna m and user u.

In this section, we introduce the STLC encoding and decoding methods for a given antenna allocation. Then, the antenna allocation strategy is considered in the sequel.

A. ENCODING AND TRANSMISSION SEQUENCE

Suppose that transmit antenna m is allocated to user u, i.e., $m \in \mathcal{M}_u$. STLC symbols $s_{m,1}$ and $s_{m,2}$ are encoded by combining two information symbols $x_{1,u}$ and $x_{2,u}$, which are weighted by channel gains between transmit antenna m and user u as

$$\begin{bmatrix} s_{m,1} \\ s_{m,2}^* \end{bmatrix} = \begin{bmatrix} h_{1,u,m}^* & -h_{2,u,m}^* \\ -h_{2,u,m} & -h_{1,u,m} \end{bmatrix} \begin{bmatrix} x_{1,u} \\ x_{2,u}^* \end{bmatrix} \quad (32)$$

and the STLC symbols are written as follows (as shown in Table 6):

$$s_{m,1} = h_{1,u,m}^* x_{1,u} - h_{2,u,m}^* x_{2,u}^*, \quad \forall m \in \mathcal{M}_u \quad (33a)$$
$$s_{m,2} = -h_{2,u,m}^* x_{1,u}^* - h_{1,u,m}^* x_{2,u}, \quad \forall m \in \mathcal{M}_u. \quad (33b)$$

At transmission time t_1, an STLC symbol s_{m,t_1} is transmitted to user u through the mth transmit antenna for all $m \in \mathcal{M}_u$, simultaneously. At the same time, other transmit antennas that are not allocated to user u generate interference

TABLE 7. Notation for STLC Received Signal $r_{n,t,u}$ at User u.

	Rx time $t=1$	Rx time $t=2$
Rx antenna $n=1$	$r_{1,1,u}$	$r_{1,2,u}$
Rx antenna $n=2$	$r_{2,1,u}$	$r_{2,2,u}$

for user u while they support other users. Denote the interference antenna set of user u by $\mathcal{M}_{\tilde{u}}$, i.e., $\mathcal{M}_{\tilde{u}} = \mathcal{M} \setminus \mathcal{M}_u$. In subsequent transmission time t_2, an STLC symbol s_{m,t_2} is transmitted to user u through the mth transmit antenna for all $m \in \mathcal{M}_u$, simultaneously. Again, other transmit antennas in set $\mathcal{M}_{\tilde{u}}$ interfere with the signal for user u. To fairly allocate the power among users [32], the transmit power of each user is limited by σ_x^2, which implies that identical time-averaged power is allocated to each user regardless of how many antennas are allocated to user. To this end, the transmitter weights (normalizes) $s_{m,t}$ with η_m. Normalization factor η_m can be readily derived as $\eta_m = 1/\sqrt{\gamma_u}$ such that $\sum_{m\in\mathcal{M}_u} \mathrm{E}\,|\eta_m s_{m,t}|^2 = \sigma_x^2$ for all t.

Denote the received signal of user u at receive antenna n at time t by $r_{n,t,u}$, as shown in Table 7. Then, the receive symbols with two receive antennas can be expressed as follows:

$$r_{1,1,u} = \frac{1}{\sqrt{\gamma_u}}\left(\sum_{m\in\mathcal{M}_u} h_{1,u,m}s_{m,1}\right) + \sum_{u'\in\mathcal{M}_{\tilde{u}}}\left(\frac{1}{\sqrt{\gamma_{u'}}}\sum_{m'\in\mathcal{M}_{u'}} h_{1,u,m'}s_{m',1}\right) + z_{1,1,u} \tag{34a}$$

$$r_{1,2,u} = \frac{1}{\sqrt{\gamma_u}}\left(\sum_{m\in\mathcal{M}_u} h_{1,u,m}s_{m,2}\right) + \sum_{u'\in\mathcal{M}_{\tilde{u}}}\left(\frac{1}{\sqrt{\gamma_{u'}}}\sum_{m'\in\mathcal{M}_{u'}} h_{1,u,m'}s_{m',2}\right) + z_{1,2,u} \tag{34b}$$

$$r_{2,1,u} = \frac{1}{\sqrt{\gamma_u}}\left(\sum_{m\in\mathcal{M}_u} h_{2,u,m}s_{m,1}\right) + \sum_{u'\in\mathcal{M}_{\tilde{u}}}\left(\frac{1}{\sqrt{\gamma_{u'}}}\sum_{m'\in\mathcal{M}_{u'}} h_{2,u,m'}s_{m',1}\right) + z_{2,1,u} \tag{34c}$$

$$r_{2,2,u} = \frac{1}{\sqrt{\gamma_u}}\left(\sum_{m\in\mathcal{M}_u} h_{2,u,m}s_{m,2}\right) + \sum_{u'\in\mathcal{M}_{\tilde{u}}}\left(\frac{1}{\sqrt{\gamma_{u'}}}\sum_{m'\in\mathcal{M}_{u'}} h_{2,u,m'}s_{m',2}\right) + z_{2,2,u} \tag{34d}$$

where the second summands in the right-hand side of (34a)–(34d) are interference terms and $z_{n,t,u}$ is AWGN with zero mean and σ_z^2 variance in the received signal $r_{n,t,u}$.

B. COMBINING SCHEME

Each user combines its own signals received over two symbol times, ignoring the interference signals. The STLC receiver of user u directly combines $\{r_{1,1,u}, r_{1,2,u}, r_{2,1,u}, r_{2,2,u}\}$ in (34a) as follows:

$$\begin{aligned} &r_{1,1,u} - r_{2,2,u}^* \\ &= \frac{1}{\sqrt{\gamma_u}}\sum_{m\in\mathcal{M}_u}\left(h_{1,u,m}s_{m,1} - h_{2,u,m}^* s_{m,2}^*\right) && (35a)\\ &\quad + \sum_{\substack{\tilde{u}\in\mathcal{U}\\ \tilde{u}\neq u}}\left(\frac{1}{\sqrt{\gamma_{\tilde{u}}}}\sum_{m'\in\mathcal{M}_{\tilde{u}}}\left(h_{1,u,m'}s_{m',1} - h_{2,u,m'}^* s_{m',2}^*\right)\right) && (35b)\\ &\quad + z_{1,1,u} - z_{2,2,u}^* && (35c)\\ &\quad - r_{2,1,u}^* - r_{1,2,u} \\ &= -\frac{1}{\sqrt{\gamma_u}}\sum_{m\in\mathcal{M}_u}\left(h_{2,u,m}^* s_{m,1}^* + h_{1,u,m}s_{m,2}\right) && (35d)\\ &\quad - \sum_{\substack{\tilde{u}\in\mathcal{U}\\ \tilde{u}\neq u}}\left(\frac{1}{\sqrt{\gamma_{\tilde{u}}}}\sum_{m'\in\mathcal{M}_{\tilde{u}}}\left(h_{2,u,m'}^* s_{m',1}^* + h_{1,u,m'}s_{m',2}\right)\right) && (35e)\\ &\quad - z_{2,1,u}^* - z_{1,2,u}. && (35f) \end{aligned}$$

The first summands (35a) and (35d) are the weighted estimate of intended signals $x_{1,u}$ and $x_{2,u}$, respectively; the second and third summands (35b) and (35e) are interference signals; and the remaining summands (35c) and (35f) are AWGN. Substituting (33a) into (35a), the intended signal $x_{1,u}$ is derived as follows:

$$\begin{aligned} &\frac{1}{\sqrt{\gamma_u}}\sum_{m\in\mathcal{M}_u} h_{1,u,m}(h_{1,u,m}^* x_{1,u} - h_{2,u,m}^* x_{2,u}^*) \\ &\quad - \frac{1}{\sqrt{\gamma_u}}\sum_{m\in\mathcal{M}_u} h_{2,u,m}^*(-h_{2,u,m}x_{1,u} - h_{1,u,m}x_{2,u}^*) \\ &= \frac{1}{\sqrt{\gamma_u}}\sum_{m\in\mathcal{M}_u}\left(|h_{1,u,m}|^2 + |h_{2,u,m}|^2\right)x_{1,u} \\ &= \sqrt{\gamma_u}x_{1,u}. \end{aligned} \tag{36}$$

Similarly, substituting (33a) into (35d), the intended signal $x_{2,u}$ is obtained as

$$\begin{aligned} &-\frac{1}{\sqrt{\gamma_u}}\sum_{m\in\mathcal{M}_u} h_{2,u,m}^*(h_{1,u,m}x_{1,u}^* - h_{2,u,m}x_{2,u}) \\ &\quad - \frac{1}{\sqrt{\gamma_u}}\sum_{m\in\mathcal{M}_u} h_{1,u,m}(-h_{2,u,m}^* x_{1,u}^* - h_{1,u,m}^* x_{2,u}) \\ &= \sqrt{\gamma_u}x_{2,u}. \end{aligned} \tag{37}$$

As seen in (36) and (37), user u, whose signals are transmitted through $|\mathcal{M}_u|$ antennas, achieves a diversity order

of $2|\mathcal{M}_u|$. The STLC receiver does not need the full CSI to combine the received signals, which we call *blind combining* [1], yet it needs an effective channel gain $\sqrt{\gamma_u}$ for maximum likelihood detection in the subsequent processing. Each user can be informed of the effective channel gain by the Tx during a signaling or training period. Note that for phase-shift-keying (PSK) symbol detection, even $\sqrt{\gamma_u}$ is not required.

C. SINR ANALYSIS

For the proposed multiuser STLC system, the received SINR is analyzed under perfect and uncertain CSI conditions.

1) SINR UNDER PERFECT CSI

To model the received SINR of users, we first rewrite the interference in (35b) as

$$(35b) = \sum_{\substack{\bar{u}\in\mathcal{U}\\ \bar{u}\neq u}} \left(\frac{1}{\sqrt{\gamma_{\bar{u}}}} \sum_{m'\in\mathcal{M}_{\bar{u}}} \Big(\big(h_{1,u,m'} h^*_{1,\bar{u},m'} + h^*_{2,u,m'} h_{2,\bar{u},m'}\big) \times x_{1,\bar{u}} + \big(h^*_{2,u,m'} h_{1,\bar{u},m'} - h_{1,u,m'} h^*_{2,\bar{u},m'}\big) x^*_{2,\bar{u}} \Big) \right)$$

and further derive it as follows:

$$(35b) = \sum_{\substack{\bar{u}\in\mathcal{U}\\ \bar{u}\neq u}} \left(\frac{1}{\sqrt{\gamma_{\bar{u}}}} \sum_{m'\in\mathcal{M}_{\bar{u}}} v_{1,\bar{u},m'} \right) \triangleq v_{1,u} \tag{38}$$

where $v_{1,\bar{u},m'}$ is the interference signal with respect to $x_{1,u}$ from transmit antenna m' that is allocated to user $\bar{u}$ and represented by a vector and matrix as

$$v_{1,\bar{u},m'} = \begin{bmatrix} h_{1,u,m'} & h^*_{2,u,m'} \end{bmatrix} \begin{bmatrix} h^*_{1,\bar{u},m'} & -h^*_{2,\bar{u},m'} \\ h_{2,\bar{u},m'} & h_{1,\bar{u},m'} \end{bmatrix} \begin{bmatrix} x_{1,\bar{u}} \\ x^*_{2,\bar{u}} \end{bmatrix} \tag{39}$$

and $v_{1,u}$ is the total interference with respect to $x_{1,u}$.

Similarly, the interference in (35e) is derived as follows:

$$-\sum_{\substack{\bar{u}\in\mathcal{U}\\ \bar{u}\neq u}} \left(\frac{1}{\sqrt{\gamma_{\bar{u}}}} \sum_{m'\in\mathcal{M}_{\bar{u}}} \left(h^*_{2,u,m'} s^*_{m',1} + h_{1,u,m'} s_{m',2} \right) \right) = \sum_{\substack{\bar{u}\in\mathcal{U}\\ \bar{u}\neq u}} \left(\frac{1}{\sqrt{\gamma_{\bar{u}}}} \sum_{m'\in\mathcal{M}_{\bar{u}}} v_{2,\bar{u},m'} \right) \triangleq v_{2,u} \tag{40}$$

where $v_{2,\bar{u},m'}$ is the interference signal with respect to $x_{2,u}$ from transmit antenna m' that is allocated to user $\bar{u}$ and represented in vector and matrix form as

$$v_{2,\bar{u},m'} = \begin{bmatrix} h_{1,u,m'} & h^*_{2,u,m'} \end{bmatrix} \begin{bmatrix} h^*_{2,\bar{u},m'} & h^*_{1,\bar{u},m'} \\ -h_{1,\bar{u},m'} & h_{2,\bar{u},m'} \end{bmatrix} \begin{bmatrix} x^*_{1,\bar{u}} \\ x_{2,\bar{u}} \end{bmatrix} \tag{41}$$

and $v_{2,u}$ is the total interference with respect to $x_{2,u}$.

Substituting (36)–(41) into (35a), the combined signals at user u are rewritten as follows:

$$r_{1,1,u} - r^*_{2,2,u} = \sqrt{\gamma_u} x_{1,u} + v_{1,u} + z_{1,1,u} - z^*_{2,2,u}, \tag{42}$$

$$-r^*_{2,1,u} - r_{1,2,u} = \sqrt{\gamma_u} x_{2,u} + v_{2,u} - z^*_{2,1,u} - z_{1,2,u}. \tag{43}$$

Noting that $(z_{1,1,u} - z^*_{2,2,u}) \sim \mathcal{CN}(0, 2\sigma_z^2)$ and $(-z^*_{2,1,u} - z_{1,2,u}) \sim \mathcal{CN}(0, 2\sigma_z^2)$ in (42) because the sum of two independent AWGNs is also an AWGN, and using that AWGN is independent of the interference signals, we can derive the received SINR of user u as follows:

$$\mathsf{SINR}_u = \frac{\gamma_u \sigma_x^2}{2\sigma_z^2 + \sigma_{v,u}^2}, \tag{44}$$

where $\sigma_{v,u}^2 = \mathrm{E}\,|v_{1,u}|^2 = \mathrm{E}\,|v_{2,u}|^2$ is the average interference power with respect to user u. From (44), we again verify that STLC achieves a diversity order of $2M$, i.e., full diversity gain. The SINR of user u clearly depends on effective channel gain γ_u and average interference power $\sigma_{v,u}^2$, and they depend on antenna allocation. Concretely, the average interference power is derived as follows (we derive it for $\mathrm{E}\,|v_{1,u}|^2$; the derivation for $\mathrm{E}\,|v_{2,u}|^2$ is the same and omitted here):

$$\begin{aligned} \sigma_{v,u}^2 &= \mathrm{E} \left| \sum_{\substack{\bar{u}\in\mathcal{U}\\ \bar{u}\neq u}} \left(\frac{1}{\sqrt{\gamma_{\bar{u}}}} \sum_{m'\in\mathcal{M}_{\bar{u}}} v_{1,\bar{u},m'} \right) \right|^2 \\ &\overset{(a)}{=} \sum_{\substack{\bar{u}\in\mathcal{U}\\ \bar{u}\neq u}} \left(\frac{1}{\gamma_{\bar{u}}} \sum_{m'\in\mathcal{M}_{\bar{u}}} \mathrm{E}\,|v_{1,\bar{u},m'}|^2 \right) \\ &\overset{(b)}{=} \sum_{\substack{\bar{u}\in\mathcal{U}\\ \bar{u}\neq u}} \left(\frac{\sigma_x^2}{\gamma_{\bar{u}}} \sum_{m'\in\mathcal{M}_{\bar{u}}} \|\boldsymbol{h}_{\bar{u},m'}\|^2 \|\boldsymbol{h}_{u,m'}\|^2 \right) \\ &\overset{(c)}{=} \sigma_x^2 \sum_{\substack{\bar{u}\in\mathcal{U}\\ \bar{u}\neq u}} \left(\frac{\sum_{m'\in\mathcal{M}_{\bar{u}}} \|\boldsymbol{h}_{\bar{u},m'}\|^2 \|\boldsymbol{h}_{u,m'}\|^2}{\sum_{m'\in\mathcal{M}_{\bar{u}}} \|\boldsymbol{h}_{\bar{u},m'}\|^2} \right) \end{aligned} \tag{45}$$

where (a) follows the fact that the interference signals caused by different transmit antennas are independent each other; (b) can be readily shown using (39); and (c) follows the definition of γ_u in (31).

Using (45) to (44), we obtain the SINR of user u as a function of the allocated channel vectors, i.e., allocated antenna set $\mathcal{M}_u$ for all $u \in \mathcal{U}$, as follows:

$$\mathsf{SINR}_u(\{\mathcal{M}_u\}) = \frac{\gamma_u \sigma_x^2}{2\sigma_z^2 + \sigma_x^2 \sum_{\substack{\bar{u}\in\mathcal{U}\\ \bar{u}\neq u}} \frac{\sum_{m'\in\mathcal{M}_{\bar{u}}} \|\boldsymbol{h}_{\bar{u},m'}\|^2 \|\boldsymbol{h}_{u,m'}\|^2}{\gamma_{\bar{u}}}}. \tag{46}$$

Now, in order to derive the lower bound of SINR, we define the strongest interference channel from user $\bar{u}$ to user u as

$$\kappa_{u,\bar{u}} \triangleq \max_{m\in\mathcal{M}_{\bar{u}}} \|\boldsymbol{h}_{u,m'}\|^2. \tag{47}$$

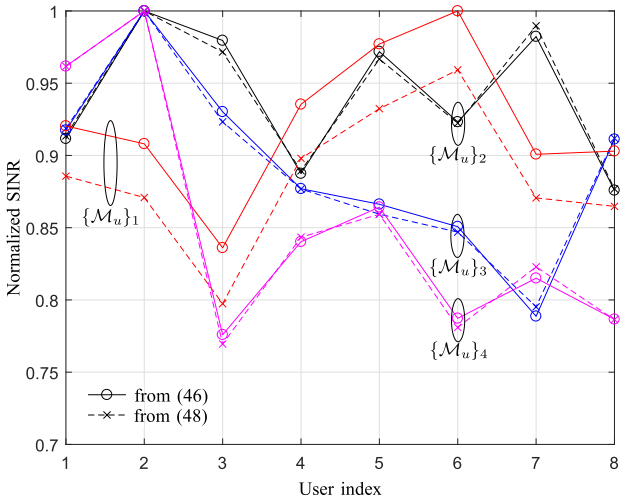

FIGURE 9. Normalized SINR evaluation for four arbitrary antenna allocation cases, namely $\{\mathcal{M}_u\}_1$, $\{\mathcal{M}_u\}_2$, $\{\mathcal{M}_u\}_3$, and $\{\mathcal{M}_u\}_4$, when $U = 8$, $|\mathcal{M}_u| = 100$, $\forall u \in \mathcal{U}$, and $\sigma_x^2/\sigma_z^2 = 20$ dB.

Using $\kappa_{u,\bar{u}}$, the lower bound of SINR in (46) can be readily derived as follows:

$$\begin{aligned}\mathsf{SINR}_u(\{\mathcal{M}_u\}) &\geq \frac{\gamma_u \sigma_x^2}{2\sigma_z^2 + \sigma_x^2 \sum_{\substack{\bar{u}\in\mathcal{U}\\ \bar{u}\neq u}} \frac{\sum_{m'\in\mathcal{M}_{\bar{u}}} \|\boldsymbol{h}_{\bar{u},m'}\|^2 \kappa_{u,\bar{u}}}{\gamma_{\bar{u}}}} \\ &= \frac{\gamma_u \sigma_x^2}{2\sigma_z^2 + \sigma_x^2 \sum_{\substack{\bar{u}\in\mathcal{U}\\ \bar{u}\neq u}} \kappa_{u,\bar{u}}} \\ &\geq \frac{\gamma_u \sigma_x^2}{2\sigma_z^2 + \sigma_x^2 (\Gamma_u - \gamma_u)} \end{aligned} \tag{48}$$

where Γ_u is the sum of channel gains from all transmit antennas to user u, i.e.,

$$\Gamma_u \triangleq \sum_{u'\in\mathcal{U}} \sum_{m\in\mathcal{M}_{u'}} \|\boldsymbol{h}_{u,m}\|^2. \tag{49}$$

Noting that Γ_u is independent of M_u, we see that the SINR lower bound (48) of user u is now decoupled from other users' SINRs, and thus, the SINR lower bound can be separately maximized by designing M_u such that it maximize γ_u.

This motivates us to consider a simple antenna allocation algorithm that intends to maximize γ_u in Section VI-D. Here, the lower bound is not necessarily tight because the antenna allocation problem is a combinatorial problem in which all the combinations have a similar tightness. Actually, the lower bound is not tight in the considered application with large $|\mathcal{M}_u|$ because in (48), the first equality holds if $|\mathcal{M}_u| = 1$ for all u and/or $\|\boldsymbol{h}_{u,m'_1}\| = \|\boldsymbol{h}_{u,m'_2}\|, \forall m'_1,\ m'_2 \in \mathcal{M}_u$, where $m'_1 \neq m'_2$; the second equality holds if $|\mathcal{M}_u| = 1$ for all u.

However, the lower bound can be used as a relevant metric in antenna allocation design, even for an STLC system with large $|\mathcal{M}_u|$, as verified in Fig. 9. Here, we show the normalized SINRs for four arbitrary antenna allocations when $U = 8$ and $|\mathcal{M}_u| = 100, \forall u \in \mathcal{U}$. The normalization is performed by the maximum SINRs. Although we observe that before normalization, the lower bound in (48) is not tight, as shown in Fig. 9, its behavior across users is almost identical to that of (46). Therefore, the SINR lower bound in (48) can be used to design antenna allocation.

2) SINR UNDER UNCERTAIN CSI

We derive the SNR of STLC under channel uncertainty from the estimate of $x_{1,u}$ (a similar procedure can be applied $x_{2,u}$ to obtain the same result). Applying the channel uncertainty model in Section V to (33a), namely,

$$s_{m,1} = \tilde{h}^*_{1,u,m} x_{1,u} - \tilde{h}^*_{2,u,m} x^*_{2,u} \tag{50a}$$
$$s_{m,2} = -\tilde{h}^*_{2,u,m} x^*_{1,u} - \tilde{h}^*_{1,u,m} x_{2,u} \tag{50b}$$

for all $m \in \mathcal{M}_u$ and $u \in \mathcal{U}$, the estimate of $x_{1,u}$ can be derived from (35a) as follows:

$$\begin{aligned}\tilde{x}_{1,u} &= \frac{1}{\sqrt{\tilde{\gamma}_u}}(r_{1,1,u} - r^*_{2,2,u}) \\ &= \frac{\gamma_u}{\tilde{\gamma}_u} x_{1,u} + \frac{1}{\tilde{\gamma}_u} \sum_{m\in\mathcal{M}_u} \left(h_{1,u,m}\epsilon^*_{1,u,m} + h^*_{2,u,m}\epsilon_{2,u,m}\right) x_{1,u} \\ &\quad + \frac{\gamma_u}{\tilde{\gamma}_u} x_{1,u} + \frac{1}{\tilde{\gamma}_u} \sum_{m\in\mathcal{M}_u} \left(h^*_{2,u,m}\epsilon_{1,u,m} - h_{1,u,m}\epsilon^*_{2,u,m}\right) x^*_{2,u} \\ &\quad + \frac{1}{\sqrt{\tilde{\gamma}}} \sum_{\substack{\bar{u}\in\mathcal{U}\\ \bar{u}\neq u}} \left(\frac{1}{\sqrt{\tilde{\gamma}_{\bar{u}}}} \sum_{m'\in\mathcal{M}_{\bar{u}}} \tilde{v}_{1,\bar{u},m'} \right) \\ &\quad + \frac{1}{\sqrt{\tilde{\gamma}_u}} \left(z_{1,1,u} - z^*_{2,2,u}\right) \end{aligned} \tag{51}$$

where $\tilde{\gamma}_u = \sum_{m\in\mathcal{M}_u} |\tilde{h}_{1,u,m}|^2 + |\tilde{h}_{2,u,m}|^2$ is the estimated effective channel gain of user u and $\tilde{v}_{1,\bar{u},m'}$ is the interference term that includes the channel uncertainty, derived similarly to (39) as

$$\tilde{v}_{1,\bar{u},m'} = \begin{bmatrix} h_{1,u,m'} & h^*_{2,u,m'} \end{bmatrix} \begin{bmatrix} \tilde{h}^*_{1,\bar{u},m'} & -\tilde{h}^*_{2,\bar{u},m'} \\ \tilde{h}_{2,\bar{u},m'} & \tilde{h}_{1,\bar{u},m'} \end{bmatrix} \begin{bmatrix} x_{1,\bar{u}} \\ x^*_{2,\bar{u}} \end{bmatrix}. \tag{52}$$

Note again that only $\tilde{\gamma}_u$ is required for user u, not the full CSI, and that even the partial CSI $\tilde{\gamma}_u$ is not required for user u if PSK constellation is used.

Comparing $x_{1,u}$ and the estimate $\tilde{x}_{1,u}$ in (51), the SINR of user u under uncertain channel presence is further derived to a function of channel uncertainty σ_ϵ^2 as (53a) at the bottom of next page (the detailed derivation is omitted here), where $S \triangleq |\mathcal{M}_u|, \forall u \in \mathcal{U}$. Clearly, when CSI is perfect, i.e., $\sigma_\epsilon^2 = 0$, the SINR in (53a) reduces to (44). Following a similar procedure to derive the lower bound of SINR when the CSI is perfect, the lower bound of SINR in (53a) is further derived as (53b), as shown at the bottom of the next page. Indeed, when the CSI is perfect, i.e., $\sigma_\epsilon^2 = 0$, the SINR lower bound in (53b) reduces to (48). Because (53b) is obviously a proportional function of γ_u, the SINR lower bound of user u can be maximized by designing $\mathcal{M}_u$ such that it maximizes γ_u, as is the case when the CSI is perfect.

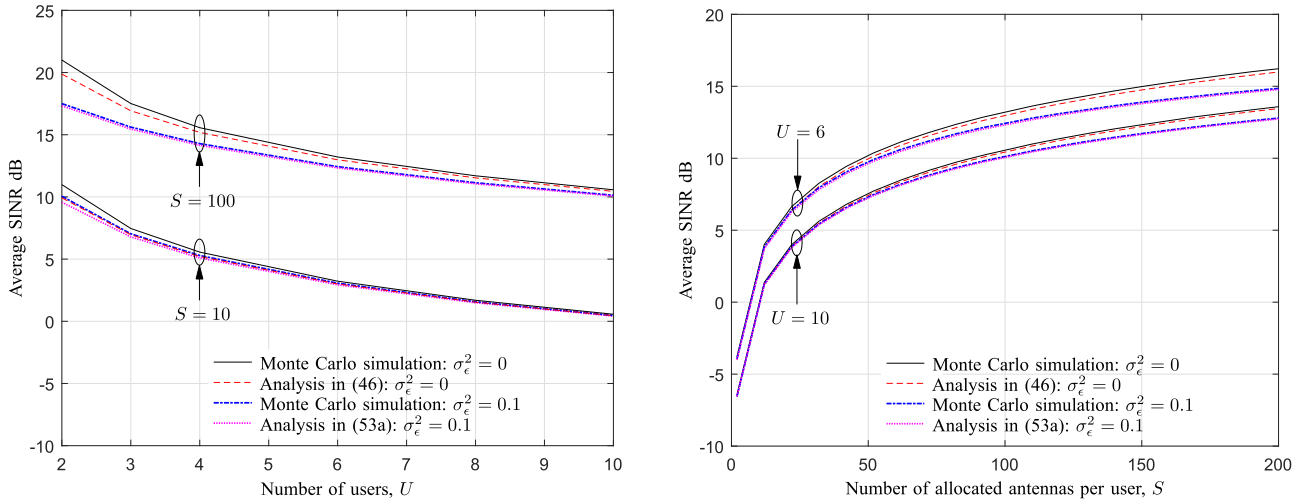

FIGURE 10. SINR evaluation when $\sigma_x^2/\sigma_z^2 = 15$ dB and $M = US$. (a) Across the number of users U when $S = 10$ and $S = 100$. (b) Across the number of antennas allocated to each user, S, when $U = 6$ and $U = 8$.

3) VERIFICATION OF ANALYSES

For the verification of the analyses in (46) and (53a), as shown at the bottom of this page, in Fig. 10, the average SINRs over users are evaluated by Monte Carlo simulation and compared with the analytical results. We assume that S antennas are allocated to each UE and $M = US$. Here, the $((u-1)S+1)$th to the (uS)th antennas are allocated to user u and $\sigma_x^2/\sigma_z^2 = 15$ dB. For the uncertain channel condition, the MSE of channel estimation is set to 0.1, i.e., $\sigma_\epsilon^2 = 0.1$.

In Fig. 10(a), the SINRs are evaluated across the number of users U when $S = 10$ and $S = 100$. These comparisons can be used to validate the analysis. As we observe in the results, the proposed STLC is robust against channel uncertainty. Furthermore, the CSI uncertainty effect, i.e., SINR degradation from the SINR when $\sigma_\epsilon^2 = 0$, decreases as the number of users U increases and the SINR decreases as U increases for a given S because of the increased interference signals. From this observation, we can conjecture that the multiuser interference affects the received SINR more severely than the channel uncertainty in an STLC system.

In Fig. 10(b), the SINRs are evaluated across S, the number of antennas allocated to each user, when $U = 6$ and $U = 10$. The comparisons show that the SINR increases as S increases for fixed U as the diversity gain increases. This observation matches expectations and the analysis is validated. Note that the channel uncertainty effect increases as S increases. The potential of diversity gain increases and the loss of the achieved diversity gain from the channel uncertainty also increases.

D. PROPOSED ANTENNA ALLOCATION ALGORITHMS

Obviously, the SINR of user u in (46) or (53a) is maximized when all transmit antennas are allocated to it, i.e., $\mathcal{M}_u = \mathcal{M}$ and $\mathcal{M}_{\bar{u}} = \emptyset$, $\forall \bar{u} \in \mathcal{U}$, where $\bar{u} \neq u$. However, other users cannot transmit at all because $\mathsf{SINR}_{\bar{u}} = 0$, $\forall \bar{u}$, which is unfair, and the average QoE becomes very poor. Using each user's SINR derived in (53a), an antenna allocation problem in order to maximize an objective function $f(\cdot)$ of the SINR is formulated as follows:

$$\{\mathcal{M}_u^*\} = \arg\max_{\{\mathcal{M}_u\}} f\left(\left\{\mathsf{SINR}_u(\{\mathcal{M}_u, \sigma_\epsilon^2\})\right\}\right) \tag{54}$$

where the objective function $f(\{q_u\})$ is a mean function, e.g.,

$$f(\{q_u\}) := \begin{cases} \frac{1}{U}\sum_u q_u, & \text{single user target} \\ \frac{1}{U}\prod_u q_u, & \text{fairness target} \\ \frac{1}{U}\sum_u [q_u - \tau_u]^+, & \text{QoE target.} \end{cases} \tag{55}$$

$$\mathsf{SINR}_u\left(\{\mathcal{M}_u\}, \sigma_\epsilon^2\right) = \frac{\left(\gamma_u + 2S\sigma_\epsilon^2\right)\sigma_x^2}{2\sigma_z^2 + \sigma_x^2\left(\frac{2\sigma_\epsilon^2(2S^2\sigma_\epsilon^2+\gamma_u)}{2S\sigma_\epsilon^2+\gamma_u} + \sum_{\substack{\bar{u}\in\mathcal{U} \\ \bar{u}\neq u}} \frac{\sum_{m'\in\mathcal{M}_{\bar{u}}}\left(\|\boldsymbol{h}_{\bar{u},m'}\|^2+2\sigma_\epsilon^2\right)\|\boldsymbol{h}_{u,m'}\|^2}{\gamma_u+2S\sigma_\epsilon^2}\right)} \tag{53a}$$

$$\geq \frac{\left(\gamma_u + 2S\sigma_\epsilon^2\right)^2\sigma_x^2}{2(E_S\Gamma_u + 2\sigma_z^2)S\sigma_\epsilon^2 + 4\sigma_x^2 S^2\sigma_\epsilon^4 + \left(2\sigma_z^2 + \sigma_x^2\Gamma_u + (1-S)\sigma_x^2\sigma_\epsilon^2\right)\gamma_u - \sigma_x^2\gamma_u^2} \tag{53b}$$

$$\triangleq \underline{\mathsf{SINR}}_u(\{\mathcal{M}_u\}, \sigma_\epsilon^2)$$

Here, τ_u is an SINR threshold that is required for the quality experience of user u and $[x]^+$ is a QoE indicator function that yields a one if $x \geq 0$, and otherwise yields a zero.

The QoE is a real value between zero and one, where a zero QoE means that no one achieves the QoE, while a QoE of one represents that all users achieves their own QoE. Here, it is worth noting that τ_u differs over users because each user has its own sensitivity and desired levels. Threshold τ_u is set to be a large value for a user who is sensitive to noisy service and, to avoid the noisy service, may subscribe an expensive service plan from a service provider. In contrast, τ_u is set to be a small value for a user who is insensitive to poor service and subscribes to an inexpensive service plan. The average QoE in (55) will be used as the performance metric in this study.

The optimization problem in (54) is clearly a nonlinear and nonconvex problem, which is formidable to solve with a closed form solution. Although (54) is a combinatorial problem, which can be optimally solved by a numerically exhaustive search, the search complexity is typically prohibitive. For example, even for the case when $|\mathcal{M}_u| = S, \forall u \in \mathcal{U}$ and $M = SU$, the number of candidates is $\binom{M}{S}\binom{M-S}{S}\cdots\binom{M-(U-1)S}{S} = M!/(S!)^U$, which increases exponentially as M increases for a given S and/or U. To reduce the computation complexity in the optimal antenna allocation search, a number of simple greedy-based algorithms are proposed based on the SINR lower bound in (53b). Maximizing the SINR lower bound of each user, i.e., $\max \underline{q}_u$, generally increases any objective function in (55). Note that the proposed algorithms focus on how many users satisfy the predetermined QoE-assured SINR target τ_u not how big the SINR achieved for each user. The average QoE improvement from the proposed algorithms is verified in the next subsection.

1) USER-DOMAIN GREEDY

Antenna allocation is performed for a specific user to achieve the specific target SINR, and then is performed for another user. In each allocation, one specific user's SINR is maximized by allocating the best transmit antenna in a greedy manner. The user selection can be implemented based on either channel quality, i.e., $\|\boldsymbol{h}_{u,m}\|$, or QoE parameter $\{\tau_u\}$. The former approach is called a channel-quality-based (CQB) approach, which is a typical resource management method in order to maximize QoE. For the latter approach, a high-QoE-first (HQF) approach that allocates antennas to a user with a higher τ_u and a low-QoE-first (LQF) approach that allocates antennas to a user with a lower τ_u are considered. The HQF approach is reasonable because a large τ_u implies a higher priority and the requirements that are relatively stringent may be fulfilled by prior antenna allocation. In contrast, the LQF is also reasonable because the users with low τ_u have a QoE that can be relatively easily satisfied, and thus, prior antenna allocation may increase the number of users who have their QoE satisfied. The numerical results (omitted in the paper) show that the HQF and LQF approaches achieve similar average QoE and slightly outperform the CQB approach.

2) ANTENNA-DOMAIN GREEDY

As pointed out at the end of Section VI-C.1, the SINR lower bound can be used to design the antenna allocation sets $\{\mathcal{M}_u\}$. Because the SINR lower bound is proportional to γ_u, we select the largest $\|\boldsymbol{h}_{u,m}\|$ for user u such that γ_u in (31) is maximized. Based on this strategy, greedy-based antenna allocation algorithms are proposed. For fairness among the users with respect to spatial resources, i.e., the number of allocated antennas, and for a tractable problem, we assume that the same number of transmit antennas is allocated to each user, i.e., $|\mathcal{M}_u| = S \triangleq M/U, \ \forall u \in \mathcal{U}$. For a simple derivation, we set $M = SU$ and S is an integer.

3) PROPOSED GREEDY-BASED ANTENNA ALLOCATION ALGORITHMS

Considering the user-domain and antenna-domain greedy strategies, the following two algorithms are proposed:

- **AG**: Determine one user and allocate S antennas in a greedy manner, and repeat the procedure until S antennas are allocated to each of the U users.
- **UG**: Determine one antenna and allocate it to a user in greedy manner, discard the user and repeat this procedure with the remaining users until there are no users remaining. Repeat this procedure until S antennas are allocated to each of the U users.

The proposed antenna allocation algorithms, namely **AG** and **UG**, are summarized in Algorithms 1 and 2, respectively.

E. SIMULATION RESULTS

For the comparison, the following three benchmarking systems were considered.

- MRTC: Using CSI at the transmitter and receiver, the MRT is performed for a larger-norm channel vector [21], [22] and MRC is applied for two received signals in order to achieve the maximum SNR [7]. As shown in Sections III and IV the MRTC outperforms STLC for a single user communication scenario if the CSI is perfect.
- GZF: Using CSI at a transmitter, space division multiple access (SDMA) precoding, i.e., the conventional zero-forcing (ZF) block-diagonalization, can be considered to support multiple users. From the SDMA precoding, multiuser channels are decomposed into multiple single user MIMO channels and multiuser interference can be eliminated. Then, the SVD approach is applied to each single-user MIMO channel, which is an optimal scheme for a single user MIMO with CSI at the transmitter and receiver in terms of the received SNR [16] and capacity [33]. This scheme scheme is termed generalized ZF (GZF) and it is relatively tractable in computational

Algorithm 1 Antenna-Greedy (AG)

1. **initial setup**: $\mathcal{M} = \{1, \ldots, M\}$, $\mathcal{U} = \{1, \ldots, U\}$, and $\mathcal{M}_u = \emptyset,\ \forall u \in \mathcal{U}$
2. **input**: channel vectors $\boldsymbol{h}_{u,m} \in \mathbb{C}^{2\times 1},\ \forall u \in \mathcal{U},\ \forall m \in \mathcal{M}$
3. **output**: set of antenna allocations, i.e., $\mathcal{M}_u,\ \forall u \in \mathcal{U}$
4. **for** $i = 1 : U$ **do**
5. find an antenna m^* that provides the strongest channel gain to the corresponding user u^*, i.e., $\{u^*, m^*\} = \arg\max_{u\in\mathcal{U}', m\in\mathcal{M}} \|\boldsymbol{h}_{u,m}\|^2$, where $\mathcal{U}' \subseteq \mathcal{U}$ is a subset of $\mathcal{U}$ constructed by either the HQF or LQF (or CQB) approaches.
6. Allocate m^* to u^*, and update $\mathcal{M}_{u^*} = \mathcal{M}_{u^*} \cup \{m^*\}$
7. **for** $j = 1 : S$ **do**
8. update the antenna set, i.e., $\mathcal{M} = \mathcal{M} \setminus \{m^*\}$
9. find an antenna m^* that provides the strongest channel gain to user u^*, i.e., $m^* = \arg\max_{m\in\mathcal{M}} \|\boldsymbol{h}_{u^*,m}\|^2$
10. Allocate m^* to u^* and update the antenna sets, i.e., $\mathcal{M} = \mathcal{M} \setminus \{m^*\}$ and $\mathcal{M}_{u^*} = \mathcal{M}_{u^*} \cup \{m^*\}$
11. **end for**
12. update user set: $\mathcal{U} = \mathcal{U} \setminus \{u^*\}$
13. **end for**

Algorithm 2 User-Greedy (UG)

1. **initial setup**, **input**, and **output** are the same as the Algorithm 1
2. **for** $i = 1 : S$ **do**
3. **for** $j = 1 : U$ **do**
4. find an antenna m^* that provides the strongest channel gain to the corresponding user u^*, i.e., $\{u^*, m^*\} = \arg\max_{u\in\mathcal{U}', m\in\mathcal{M}} \|\boldsymbol{h}_{u,m}\|^2$, where $\mathcal{U}' \subseteq \mathcal{U}$ is a subset of $\mathcal{U}$ constructed by either HQF or LQF (or CQB) approaches.
5. Allocate m^* to u^* and update the sets, i.e., $\mathcal{M}_{u^*} = \mathcal{M}_{u^*} \cup \{m^*\}, \mathcal{U} = \mathcal{U} \setminus \{u^*\}, \mathcal{M} = \mathcal{M} \setminus \{m^*\}$
6. **end for**
7. Initialize the user set as $\mathcal{U} = \{1, \ldots, U\}$
8. **end for**

complexity for a massive MIMO system compared to other multiuser MIMO schemes, such as dirty paper coding and vector perturbation schemes, [34].

- STLC-random: For a multiuser STLC system, S transmit antennas are randomly allocated to each user. The STLC-random represents a multiuser STLC system without antenna allocation, which is the QoE lower bound of a multiuser STCL system with antenna allocation.

Throughout the simulation, CQB is used for user selection with AG and UG. As the performance metric for the comparison, the average QoE in (55) is used.

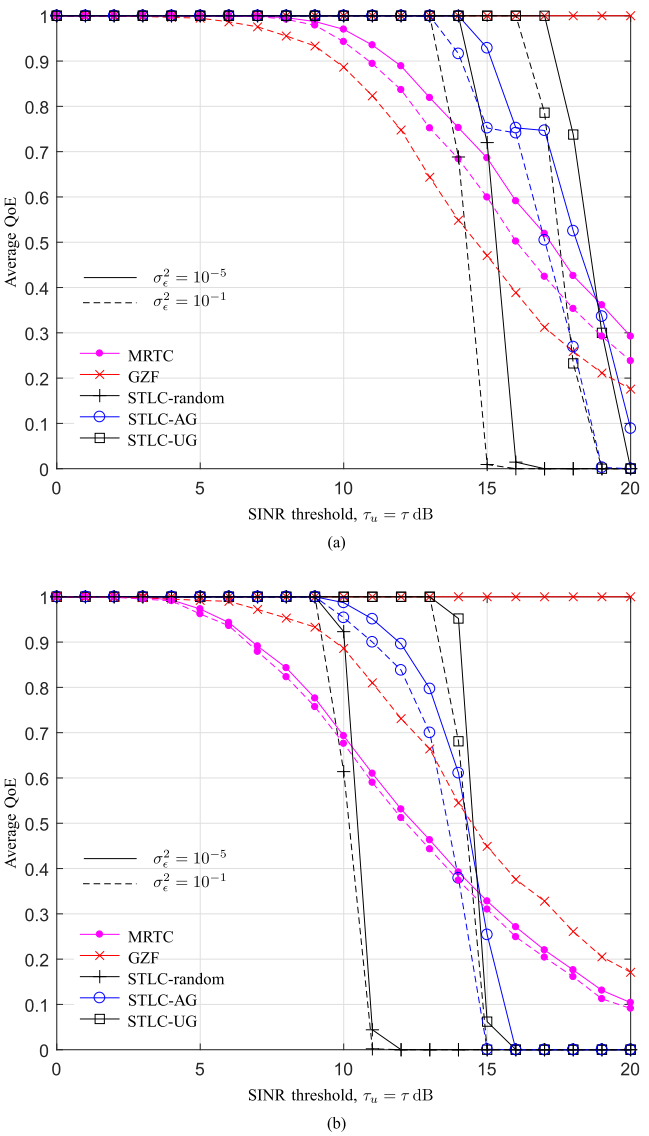

FIGURE 11. QoE across SINR threshold τ when $\sigma_x^2/\sigma_z^2 = 20$ dB, $S = 100$, and $M = SU$. (a) $U = 4$. (b) $U = 10$.

1) HOMOGENEOUS USER PROFILE

In Fig. 11(a), a homogeneous user profile is considered for four users. In the homogeneous user profile scenario, the target SINRs of all users are set to be equal, i.e., $\tau_u = \tau$ for all $u \in \mathcal{U}$. For channel uncertainty in the evaluation, two MSE values are considered, namely $\sigma_\epsilon^2 = 0.1$ for very uncertain CSI and $\sigma_\epsilon^2 = 10^{-5}$ for accurate CSI. The MRTC and GZF schemes show different QoE-τ trends from those of STLC-based methods. Specifically, GZF achieves the best QoE performance when the CSI is accurate. Even though the GZF scheme achieves the best QoE when CSI is perfect, its computational complexity $\mathcal{O}(M^3)$ is much greater than $\mathcal{O}(M)$, which is the complexity order of the STLC-based methods. However, the GZF performance deteriorates severely when the CSI is uncertain because of the failure to eliminate multiuser interference signals. A similar

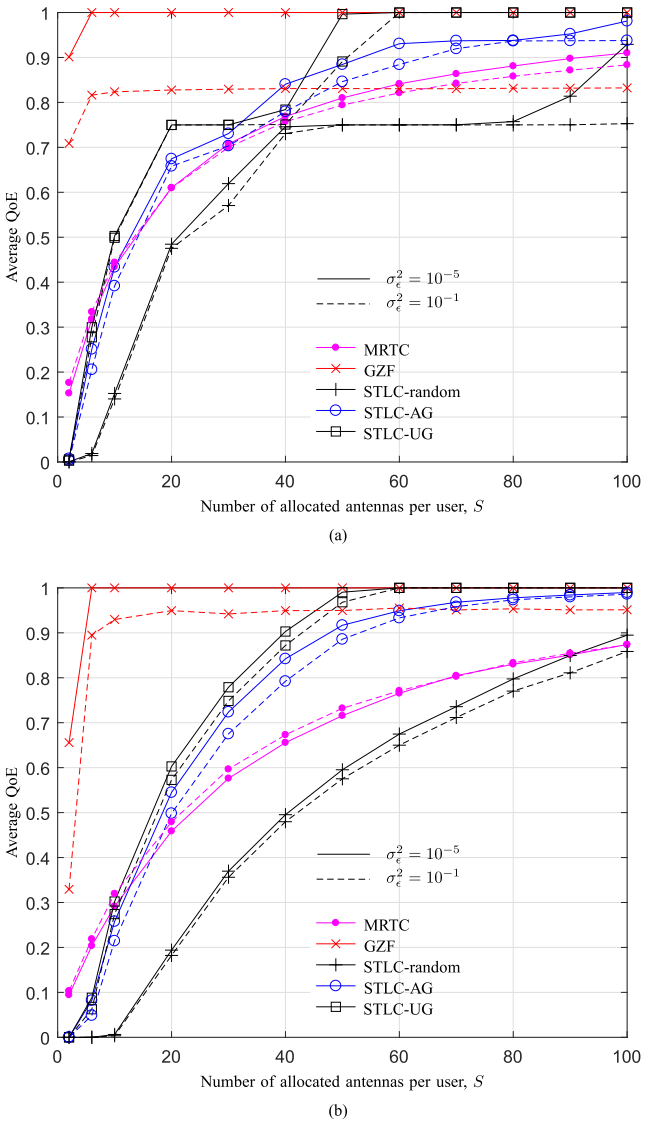

FIGURE 12. QoE across the number of allocated antennas per user, S, when $\sigma_x^2/\sigma_z^2 = 20$ dB and $M = SU$. (a) $U = 4$. (b) $U = 10$.

observation regarding the severe performance degradation caused by uncertain CSI in nonlinear processing is shown in Section V. All schemes except for the GZF scheme ignore multiuser interference signals in the pre/post-processing design. Thus, the performance depends on how much the intended channel gain is improved. Observing the largest τ with perfect QoE ($= 1$), when CSI is uncertain, the proposed STLC-based methods outperform MRTC and GZF. In particular, the STLC-UG scheme achieves the best QoE.

In Fig. 11(b), 10 users, i.e., $U = 10$, are considered. As U increases, generally, the QoE decreases because of the increase of multiuser interference (except for the GZF scheme, which manages this interference), and similar results are observed as when $U = 4$ in Fig. 11(a). The performance degradation from the CSI uncertainty is relatively small (except for the GZF scheme) because the multiuser interference is dominant. In a moderate target SINR region (lower than 14 dB), the proposed STCL-UG achieves the best QoE.

2) MIXTURE QoE SCENARIO

In Fig. 12, a mixture of different target SINRs for different users, i.e., a heterogenous user profile scenario, is considered as follows: $\{\tau_1 = 5\,\text{dB}, \tau_2 = 7\,\text{dB}, \tau_3 = 10\,\text{dB}, \tau_4 = 15\,\text{dB}\}$ for the simulation shown in Fig. 12(a) and $\{\tau_u = (u+1)\,\text{dB}\}$ for the simulation shown in Fig. 12(b). For a fixed τ_u, the average QoE is evaluated across the number of allocated antennas per user, i.e., S. In the mixture QoE scenario, the proposed STLC-UG achieves a QoE of one, like the GZF scheme when S is greater than about 50. Similarly, we can conjecture that an STLC-AG also achieves a QoE of one if S keeps increasing. This is because the effective channel gain from antenna allocation increases as S increases. Furthermore, when the CSI is uncertain and S is large, the STLC-UG outperforms even the GZF scheme. Here, it is worth emphasizing again that the computational complexity order of the STLC-based schemes is linear in S, i.e., $\mathcal{O}(M) = \mathcal{O}(S)$ for a given number of users. Therefore, the proposed STLC-based schemes can be a relevant potential candidate for a massive MIMO system supporting multiple users.

VII. CONCLUSION

In this study, we verified the benefits of the proposed full-spatial-diversity-achieving STLC over MRTC and/or MEB schemes as follows: i) low computational complexity at the transceiver, ii) no or partial CSI required at the receiver, and iii) robustness against CSI uncertainty. With those benefits, the proposed STLC scheme achieves comparable performance to MRTC and MEB schemes. The STLC scheme was then applied to a system supporting multiple users. Considering multiuser interferences and channel uncertainty, the SINR of each user and its lower bound were analyzed and the analyses were numerically verified. To improve SINR and QoE, we proposed algorithms that allocate transmit antennas to each user based on the SINR lower bound. Through rigorous simulation, it was validated that the multiuser STLC with the proposed antenna allocation is robust against channel uncertainty and can achieve the best QoE if the number of transmit antennas is sufficiently large. The results in this study showed that the STLC can be a potential candidate for an M-by-2 (multiuser) massive MIMO systems. The practical implementation of the basic idea of STLC in this study, using digital signal processors (DSPs) and/or field programmable gate arrays (FPGAs), is one of the interesting topics for further study.

REFERENCES

[1] J. Joung, "Space-time line code," *IEEE Access*, to be published. [Online]. Available: http://ieeexplore.ieee.org/stamp/stamp.jsp?arnumber=8119932
[2] V. Tarokh, N. Seshadri, and A. R. Calderbank, "Space-time codes for high data rate wireless communication: Performance criterion and code construction," *IEEE Trans. Inf. Theory*, vol. 44, no. 2, pp. 744–765, Mar. 1998.

[3] S. M. Alamouti, "A simple transmit diversity technique for wireless communications," *IEEE J. Sel. Areas Commun.*, vol. 16, no. 8, pp. 1451–1458, Oct. 1998.
[4] V. Tarokh, H. Jafarkhani, and A. R. Calderbank, "Space-time block codes from orthogonal designs," *IEEE Trans. Inf. Theory*, vol. 45, no. 5, pp. 1456–1467, Jul. 1999.
[5] V. Tarokh, H. Jafarkhani, and A. R. Calderbank, "Space-time block coding for wireless communications: Performance results," *IEEE J. Sel. Areas Commun.*, vol. 17, no. 3, pp. 451–460, Mar. 1999.
[6] J. Choi and J. Joung, "Artificial-noise-aided space-time line code for secure MIMO communications," *IEEE J. Sel. Areas Commun.*, submitted for publication.
[7] W. C. Jakes, *Microwave Mobile Communications*. New York, NY, USA: Wiley, 1994.
[8] C. Chayawan and V. A. Aalo, "Average error probability of digital cellular radio systems using MRC diversity in the presence of multiple interferers," *IEEE Trans. Wireless Commun.*, vol. 2, no. 5, pp. 860–864, Sep. 2003.
[9] S. Roy and P. Fortier, "Maximal-ratio combining architectures and performance with channel estimation based on a training sequence," *IEEE Trans. Wireless Commun.*, vol. 3, no. 4, pp. 1154–1164, Jul. 2004.
[10] W. M. Gifford, M. Z. Win, and M. Chiani, "Diversity with practical channel estimation," *IEEE Trans. Wireless Commun.*, vol. 4, no. 4, pp. 1935–1947, Jul. 2005.
[11] K. S. Ahn and R. W. Heath, "Performance analysis of maximum ratio combining with imperfect channel estimation in the presence of cochannel interferences," *IEEE Trans. Wireless Commun.*, vol. 8, no. 3, pp. 1080–1085, Mar. 2009.
[12] H. Huh, G. Caire, H. C. Papadopoulos, and S. A. Ramprashad, "Achieving 'massive MIMO' spectral efficiency with a not-so-large number of antennas," *IEEE Trans. Wireless Commun.*, vol. 11, no. 9, pp. 3226–3239, Sep. 2012.
[13] E. G. Larsson, O. Edfors, F. Tufvesson, and T. L. Marzetta, "Massive MIMO for next generation wireless systems," *IEEE Commun. Mag.*, vol. 52, no. 2, pp. 186–195, Feb. 2014.
[14] X. Guo, S. Chen, J. Zhang, X. Mu, and L. Hanzo, "Optimal pilot design for pilot contamination elimination/reduction in large-scale multiple-antenna aided OFDM systems," *IEEE Trans. Wireless Commun.*, vol. 15, no. 11, pp. 7229–7243, Nov. 2016.
[15] J. Fang, X. Li, H. Li, and F. Gao, "Low-rank covariance-assisted downlink training and channel estimation for FDD massive MIMO systems," *IEEE Trans. Wireless Commun.*, vol. 16, no. 3, pp. 1935–1947, Mar. 2017.
[16] S. Zhou and G. B. Giannakis, "Optimal transmitter eigen-beamforming and space-time block coding based on channel mean feedback," *IEEE Trans. Signal Process.*, vol. 50, no. 10, pp. 2599–2613, Oct. 2002.
[17] R. W. Heath, S. Sandhu, and A. Paulraj, "Antenna selection for spatial multiplexing systems with linear receivers," *IEEE Commun. Lett.*, vol. 5, no. 4, pp. 142–144, Apr. 2001.
[18] S. Yan, N. Yang, R. Malaney, and J. Yuan, "Transmit antenna selection with alamouti coding and power allocation in MIMO wiretap channels," *IEEE Trans. Wireless Commun.*, vol. 13, no. 3, pp. 1656–1667, Mar. 2014.
[19] J. Joung and S. Sun, "Two-step transmit antenna selection algorithms for massive MIMO," in *Proc. IEEE Int. Conf. Commun. (ICC)*, Kuala Lumpur, Malaysia, May 2016, pp. 1–5.
[20] P. Gao and C. Tepedelenlioğlu, "SNR estimation for nonconstant modulus constellations," *IEEE Trans. Signal Process.*, vol. 53, no. 3, pp. 865–870, Mar. 2005.
[21] T. L. Marzetta, "Noncooperative cellular wireless with unlimited numbers of base station antennas," *IEEE Trans. Wireless Commun.*, vol. 9, no. 11, pp. 3590–3600, Nov. 2010.
[22] C. Shepard *et al.*, "Argos: Practical many-antenna base stations," in *Proc. ACM Int. Conf. Mobile Comput. Netw.*, New York, NY, USA, Aug. 2012, pp. 53–64.
[23] A. Edelman, "Eigenvalues and condition numbers of random matrices," *SIAM J. Matrix Anal. Appl.*, vol. 9, no. 4, pp. 543–560, 1988.
[24] A. Goldsmith, *Wireless Communications*. Cambridge, NY, USA: Cambridge Univ. Press, 2005.
[25] G. H. Golub and C. F. Van Loan, *Matrix Computations*, 3rd ed. Baltimore, MD, USA: The Johns Hopkins Univ. Press, 1996.
[26] Z. Jiang, A. F. Molisch, G. Caire, and Z. Niu, "Achievable rates of FDD massive MIMO systems with spatial channel correlation," *IEEE Trans. Wireless Commun.*, vol. 14, no. 5, pp. 2868–2881, May 2015.
[27] L. You, X. Gao, X. G. Xia, N. Ma, and Y. Peng, "Pilot reuse for massive MIMO transmission over spatially correlated Rayleigh fading channels," *IEEE Trans. Wireless Commun.*, vol. 14, no. 6, pp. 3352–3366, Jun. 2015.
[28] S. Mumtaz, J. Rodriguez, and L. Dai, *mmWave Massive MIMO: A Paradigm for 5G*. London, U.K.: Academic, 2016.
[29] J.-P. Kermoal, L. Schumacher, K. I. Pedersen, P. E. Mogensen, and F. Frederiksen, "A stochastic MIMO radio channel model with experimental validation," *IEEE J. Sel. Areas Commun.*, vol. 20, no. 6, pp. 1211–1226, Aug. 2002.
[30] M. Matthaiou, M. R. McKay, P. J. Smith, and J. A. Nossek, "On the condition number distribution of complex Wishart matrices," *IEEE Trans. Commun.*, vol. 58, no. 6, pp. 1705–1717, Jun. 2010.
[31] A. Goldsmith, S. A. Jafar, N. Jindal, and S. Vishwanath, "Capacity limits of MIMO channels," *IEEE J. Sel. Areas Commun.*, vol. 21, no. 5, pp. 684–702, Jun. 2003.
[32] J. Joung and S. Sun, "Energy efficient power control for distributed transmitters with ZF-based multiuser MIMO precoding," *IEEE Commun. Lett.*, vol. 17, no. 9, pp. 1766–1769, Sep. 2013.
[33] G. C. Raleigh and J. M. Cioffi, "Spatio-temporal coding for wireless communication," *IEEE Trans. Commun.*, vol. 46, no. 3, pp. 357–366, Mar. 1998.
[34] J. Joung *et al.*, "Capacity evaluation of various multiuser MIMO schemes in downlink cellular environments," in *Proc. IEEE Int. Symp. Personal, Indoor Mobile Radio Commun. (PIMRC)*, Helsinki, Finland, Sep. 2006, pp. 1–5.

JINGON JOUNG (S'03–M'07–SM'15) received the B.S. degree in radio communication engineering from Yonsei University, Seoul, South Korea, in 2001, and the M.S. and Ph.D. degrees in electrical engineering and computer science from the Korea Advanced Institute of Science and Technology (KAIST), Daejeon, South Korea, in 2003 and 2007, respectively.

He was a Scientist with the Institute for Infocomm Research, Agency for Science, Technology and Research, Singapore. He was a Post-Doctoral Research Scientist with KAIST, and a Post-Doctoral Fellow with UCLA, CA, USA. In 2016, he joined Chung-Ang University, Seoul, where he is currently a Professor with the School of Electrical and Electronics Engineering and a Principal Investigator of the Wireless Systems Laboratory. His research activities are in the area of multiuser systems, multiple-input multiple-output communications, and cooperative systems, and his current research area/interest includes energy-efficient ICT, IoT, and machine learning algorithms.

Dr. Joung was a recipient of the First Prize at the Intel-ITRC Student Paper Contest in 2006. He has been serving on the Editorial Board of the *APSIPA Transactions on Signal and Information Processing* since 2014. He served as the Guest Editor of IEEE Access for special section "Recent Advanced in Full-Duplex Radios and Networks" in 2016. He was recognized as the Exemplary Reviewers in 2012 from the IEEE Communications Letters, and in 2012 and 2013, from the IEEE Wireless Communications Letters.